2 CHAPTER TWO:

CLONING, NUCLEOTIDE SEQUENCES AND RNA SYNTHESIS OF MUTATED *P. FALCIPARUM* HEXOSE TRANSPORTERS

2.1 Introduction

For glucose transport, mammalian cells employ Na^+-dependent co-transporters and the simple facilitative uniporters. The facilitative glucose transporters (GLUT1-5) are the most thoroughly studied of all facilitated diffusion transport systems. They are energy-independent systems that only transport down a concentration gradient, and are therefore most effective in environments where continual exposure to high concentrations of substrate is experienced (Mueckler, 1994).

Indirect approaches such as glycosylation-scanning mutagenesis (Hresko *et al*, 1994), cysteine-scanning mutagenesis (Olsowski *et al*, 2000) and site-directed mutagenesis (Seatter *et al*, 1998) have been applied extensively to GLUT1 and have provided insight into its secondary and tertiary structure. Mueckler *et al* (1985) proposed a 12 transmembrane helical model for the glucose transporter from human HepG2 hepatoma cells. Two alternative topographic assignments of GLUT1 have since been proposed. One favours a secondary structure with 16 β-strands resembling the bacterial porin protein (Fischbarg *et al*, 1993). The other favours an α-helix-β-strand transmembrane structure with 14 membrane spanning segments (Ducarme *et al*, 1996). Studies conducted by Alvarez *et al* (1987) using Fourier transform infrared (FT-IR) spectroscopy revealed that more than 80% of the polypeptide backbone of GLUT1 is accessible to solvent which is consistent of a pore like structure. Circular dichroism measurements have indicated that the protein is made largely of α-helices (70%) with 20% β-turns and 10% random coil (Chin *et al*, 1986). These findings support the 12 α-helical model. The results obtained from a glycosylation scanning mutagenesis study conducted by Hresko *et al* (1994) also strongly supported this

model. A potential site of *N*-linked glycosylation (Asn-X-Ser or Thr, where X is any amino acid) was identified at Asn^{45} for the 12 helical model (Muekler *et al*, 1985).

There are 10 invariant amino acid residues in all members of the sugar transporter family (Kayano *et al*, 1990). Humans, rats, mice, pigs and rabbits all have GLUT1s that have 492 residues and are more than 97% identical in sequence (Mueckler, 1994). For the proposed 12 helical model, 5 of the 12 transmembrane helices (helices 3, 5, 7, 8 and 11) are capable of forming amphipathic α-helices and are predicted to form an aqueous pore (Mueckler and Makepeace, 1999). Most structure/ function studies concerning facilitated glucose transporters have been conducted on GLUT1 mainly on the 5 proposed amphipathic helices and conserved amino acids. As a result a few interesting details have appeared in the literature in accordance with the proposed 12 helical model.

Tryptophan is a rare amino acid in proteins and usually plays a role in structure and catalytic activity. GLUT1 has 6 Tryptophan residues, three of which are conserved in GLUT1-5. In a study conducted by Garcia *et al* (1992) the tryptophan residues in GLUT1 were changed to either glycine or leucine residues. Transport was decreased in the Trp-388 (helix 10) and Trp-412 (helix 11) mutants but was unaltered in all the other mutants. Proline 385 in helix 10 when mutated to isoleucine resulted in the transporter being fixed in the inward facing conformation (Tamori *et al*, 1994). Cysteine 429 within the 6^{th} external loop, and cysteine 207 at the beginning of the large intracellular loop connecting helix 6 and 7 was predicted to contribute towards the transport of glucose (Wellner *et al*, 1994). Glutamine 161 (helix 5) was predicted to form part of the exofacial ligand binding site of GLUT1 and when mutated to leucine or asparagine the transport activity is reduced by 50% and 10%, respectively (Mueckler *et al*, 1994). Proline residues in helix 6 and 10 were investigated with point mutations. Proline residues in GLUT1, conserved in all human glucose transporter isoforms, were mutated to either alanine or the corresponding amino acid in GLUT2. The results revealed that no single proline residue was essential for transport activity. However proline substitutions in helix 10 to neutral residues completely abolished transport of 2-deoxy-D-glucose. Therefore the proline residues cis-trans shift is not

important for transporter activity but rather the chemical compositions of the amino acid side chains (Wellner *et al*, 1995).

Interest has been centred on the differences in transportation of glucose and fructose, and on amino acids responsible for the selectivity of substrate. For instance, the mammalian transporters GLUT1, 3 and 4 transport glucose only and all contain a conserved QLS motif in helix 7, whereas GLUT2 and 5 are capable of fructose transport and do not have this conserved motif (Table 2.1; Seatter *et al*, 1998). Arbuckle *et al* (1996) used chimaeric GLUT2/GLUT3 constructs to establish the site responsible for fructose transport. GLUT3 constructs containing the GLUT2 helix 7 segment were able to transport fructose to some degree (Arbuckle *et al*, 1996). Seatter *et al* (1998) took this idea one step further and prepared two mutants in which QLS of GLUT3 was substituted with the corresponding HVA from GLUT2 and *vice versa*. Their results suggested that the QLS motif in helix 7 is in some way responsible for the ability of GLUT 1, 3 and 4 to transport D-glucose and their inability to transport fructose.

Table 2.1: Sequence alignments of different hexose/ glucose transporter putative transmembrane helix 7 segments. The ability of each transporter to transport fructose and/ or glucose is indicated. Human glucose transporters have a common QLS motif (highlighted in bold) whereas human fructose transporters do not, and neither do the hexose transporters from the other organisms mentioned (Kayano *et al*, 1990; Barret *et al*, 1998). GLUT1-5, mammalian glucose transporters 1-5; PfHT1, *Plasmodium falciparum* hexose transporter; THT1, *Trypanosome brucei* hexose transporter one.

Transporter	Sequence	Transport of:
GLUT1	279 **QLS**QQLSGINA	Glucose
GLUT2	311 HVAQQFSGING	Glucose (low affinity) and Fructose
GLUT3	277 **QLS**QQLSGINA	Glucose
GLUT4	295 **QLS**QQLSGINA	Glucose
GLUT5	285 MGGQQLSGVNA	Fructose
PfHT1	302 SGLQQFTGINV	Glucose and Fructose
THT1	311 AGTLQLTGINA	Glucose and Fructose

Interest has also been placed on the 5 helices that are capable of forming amphipathic structures and therefore predicted to lie close to one another to form an aqueous core. Work involving GLUT1 helix 7 has established its role in exofacial ligand binding. Mutations in this helix, more specifically glutamine 282, resulted in reduced affinity for outside site-specific ligands 2-*N*-4-(1-azi-2,2,2-trifluoroethyl) benzoyl-1,3-bis(D-mannos-4-yloxy)-2-propylamine (ATB-BMPA) and 4,6-*O*-ethylidene-D-glucose indicating its possible role in substrate binding (Seatter *et al*, 1998; Hashiramoto *et al*, 1992). A cysteine-scanning mutagenesis study conducted by Hruz and Mueckler (1999) on helix 7 showed that cysteine replacement at positions near the exofacial side of the cell membrane, namely Gln^{282}, Gln^{283}, Ile^{287}, Ala^{289}, Val^{290} and Phe^{291} produced transporters that were inhibited by *p*-chloromercuribenzene sulfonate (pCMBS), which binds extracellularly. This provided evidence to support the hypothesised accessibility of this helix to the external solvent. The authors also proposed a possible model for GLUT1 helix packaging (Figure 2.1B; Hruz and Mueckler, 1999).

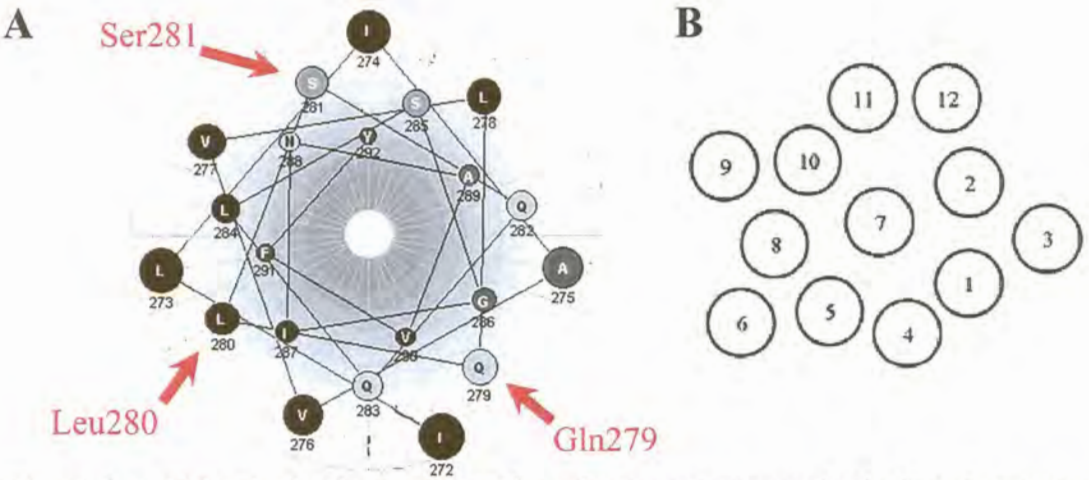

Figure 2.1: Helical wheel representation of transmembrane helix 7 and proposed model for GLUT1 helix packaging (Hruz and Mueckler, 1999). Figure A: Helix 7 wheel. The amino acids indicated by arrows, Gln279; Leu280 and Ser281, correspond to the amino acids Ser 302; Gly303 and Leu304 in PfHT1 focused on in this study. The schematical representation enables one to note the proximity of these amino acids to the exterior medium. **Figure B:** Proposed model for helical packaging in GLUT1. This view allows one to notice the proximity of each helix to its neighbours.

The recent discovery of the *P. falciparum* hexose transporter PfHT1, which is expressed in the asexual stage of the parasite, has opened up a whole new pathway for drug target development (Woodrow *et al*, 1999). This discovery is useful since the

intra-erythrocytic malaria parasite depends on glucose from its host for energy, which is metabolised via glycolysis (Kirk *et al*, 1996). Parasite-infected erythrocytes exhibit an increase in glucose uptake when compared to uninfected erythrocytes and it is believed that PfHT1 is the major hexose transporter for the intraerythrocytic parasites (Krishna *et al*, 2000). Work done by Woodrow *et al* (1999) revealed that *PfHT1* is a single copy gene with no close homologues within the translated region when compared to other related and non-related species. Expression of *PfHT1* peaks 8h after invasion, which is consistent with an increase in glucose consumption as ring forms mature to trophozoites. PfHT1 has a relatively high affinity for hexoses with a ten-fold higher affinity for D-glucose compared to the mammalian erythrocyte and endothelial located glucose transporter GLUT1 (Woodrow *et al*, 1999).

Analyses of substrate specificity of PfHT1 expressed in *Xenopus laevis* oocytes have shown that fructose binds in a furanose conformation and glucose in a pyranose conformation. Helix 5 appears to be involved in fructose transport, since this is ablated by mutation of Q169 to asparagine, which lies within helix 5 (Woodrow *et al*, 2000). The most important sites on the glucose molecule for interaction with PfHT1 appear to be C-3 and C-4 (Woodrow *et al*, 1999), and for GLUT1 the most important appear to be the ring oxygen and hydroxyls at C-1 and C-3, with a lesser contribution from C-4 and C-6 (Baldwin, 1992).

Although phylogenically unrelated to both mammals and *Plasmodium* species, kinetoplastid organisms (*Trypanosoma* and *Leishmania* species) also require glucose at certain stages of their life cycles. Protozoa of the order kinetoplastida habitat many areas and several species are important parasites of humans. Many glucose transporters from kinetoplastids have been cloned and they all belong to the major facilitator superfamily. Kinetoplastida include African trypanosomes, which cause sleeping sickness in humans (*Trypanosoma brucei*) and South American trypanosomes such as *Trypanosoma cruzi*, which causes Chagas' disease (Tetaud *et al*, 1997).

African *Trypanosoma* are transmitted by tsetse flies or other biting insects and live free in the blood, central nervous system and other tissue fluids. *T. cruzi* by contrast

live intracellularly in their mammalian hosts (Barrett *et al*, 1998). Two separate isoforms of the trypanosome hexose transporter (THT1 and THT2) were isolated from *T. brucei* by Bringaud and Baltz (1993). THT1 is the most abundantly expressed isoform in the bloodstream form parasite. The trypanosome glucose transporters have features that distinguish them from the mammalian glucose transporters. These include insensitivity to cytochalasin B and the ability to transport D-fructose. Also the long intracellular loop between helix 6 and 7 in GLUT1 is not present in trypanosomal glucose transporters (Barrett *et al*, 1998). The most important hydrogen bonding sites on THT1 appear to be C-3 and C-4. The K_m for D-glucose of the *T. brucei* blood stream form is 0.49-1.18 mM (Barrett *et al*, 1998; Tetaud *et al*, 1997) and the K_i for D-fructose is approximately 2.56 mM (Tetaud *et al*, 1997). Kinetoplastid organisms share many common challenges during their mammalian parasitic stages with the malaria parasite. Therefore sugar transporters of the kinetoplastids offer an exceptional model to study the ways in which the sugar transporters have evolved to meet different environmental challenges (Tetaud *et al*, 1997). A correlation can be made between THT1 and PfHT1 in how they differ from GLUT1, which could lead to an understanding of the significance of their differences. PfHT1 was mutated to contain a motif from THT1 that could contribute towards the ability of the two parasitic glucose transporters to transport fructose. This motif corresponds to the QLS motif in GLUT1 (Table 2.1, Figure 2.1A) that is conserved in the mammalian GLUT glucose transporters and is thought to play a part in glucose/ fructose recognition.

2.2 Materials and methods

2.2.1 Primer design

Primers were designed to incorporate point mutations within helix 7 (302SGL motif). This motif was mutated to the *T. brucei* hexose transporter THT1 helix 7 motif (311AGT) since THT1 also transports glucose and fructose. Four sets of primers were designed: three complementary sets for incorporation of the point mutations and one set for the extension of the full-length gene (Table 2.2). Primers HTKB1&2 lie at opposite ends of the full-length gene and include the start and stop codons

respectively. The primers also contain *Bgl*II restriction sites at their 5' ends for cloning into the *X. laevis* expression vector pSP64T. Upon delivery, primers were diluted in double distilled water to stocks of 80 µM concentrations.

Table 2.2: Sequences of primers used for PCR 1 and 2. Primers are in the 5' to 3' direction. Numbering (1 and 2) refers to forward and reverse primers respectively. Mutated bases are indicated in bold italics. Start and stop codons are in bold. The Kozak sequence in the HTKB1 primer is in italics. Restriction sites are underlined.

Primer name	Primer sequence (5'→3')	Restriction sites
AGT1	GGATGTTTG***C***TA***G***CTGGT***AC***ACAACAATTTACAGG	*NheI*
AGT2	CCTGTAAATTGTTGT***GT***ACCAG***C***TA***G***CAAACATCC	
AGL1	GGATGTTTG***C***TA***G***CTGGT***C***T***G***CA***G***CAATTTACAG	*NheI*, *PstI*
AGL2	CTGTAAATTG***C***TG***C***A***G***ACCAG***C***TA***G***CAAACATCC	
SGT1	GGATGTTTG***C***TATCTGGT***ACC***CAACAATTTACAG	*KpnI*
SGT2	CTGTAAATTGTTG***GGT***ACCAGATA***G***CAAACATCC	
HTKB1	ACGTACAGATCT*CACC***ATG**ACGAAAAGTTCGAAAG	*BglII*
HTKB2	ACGTACAGATCT**TCA**TACAACCGACTTGGTC	

Table 2.3: Characteristics of the primers used to synthesise mutant S302A and L304T constructs.

Primer	AGL1/AGL2	SGT1/SGL2	HTKB1	HTKB2
Length	34	34	35	31
%A/T	56	58	57	55
Tm Genosys[1]	76.6	72.6	75.6	71.4
Calculated Tm[2]	68.2	67.0	68.4	66.8

[1] Melting temperature (Tm) supplied with the primers and calculated by Sigma-Genosys.

[2] Tm is calculated according to the following equation (Rychlik *et al*, 1990):

$69.3 + (0.41 \times \%GC) - 650/length$

The primers that produced the mutations were designed to contain the mutated area in the middle of the primer and a restriction site over or near the mutated area that would be used to confirm the presence of the mutation without sequencing. All primers were

synthesised by Sigma-Genosys Ltd, London, UK. The Tm of each primer was calculated. The characteristics of the primers are summarised in Table 2.3.

2.2.2 Polymerase Chain Reaction (PCR) for the construction of helix 5 and helix 7 mutations

2.2.2.1 PCR 1: construction of mutants

The Polymerase Chain Reaction for the production of the S302A and L304T mutants had to be optimised for each set of primers (mutant 302SGL→AGT was already constructed by Charles Woodrow). Wild-type PfHT1 in the pSP64T *X. laevis* expression vector at a concentration of 200 ng/µl was used as template in a 1:1000 dilution (Woodrow *et al*, 1999). Reaction volumes of 25 µl for each reaction were set up under optimised reaction conditions as summarised in Table 2.4.

Table 2.4: Optimised reaction conditions for the synthesis of the S302A and L304T mutants in 25 µl reaction volumes.

Reaction component	Final in 25 µl
Cloned Pfu reaction buffer 10×	1×
dNTP 2 mM each	0.16 mM each
$MgCl_2$ 25 mM	2 mM
Mutation-inducing primer (AGL1, SGT1, AGL2 or SGT2)	10 pmol
Gene primer (HTKB1 or HTKB2)	10 pmol
Cloned Pfu DNA Polymerase 2500 units/ml	0.625 Units

The DNA polymerase Pfu from the hyperthermophilic archae *Pyrococcus furiosis* (Stratagene, USA) was used. It has 3' to 5' exonuclease proofreading activity that enables the polymerase to correct nucleotide miss-incorporation errors but lacks extendase activity, which results in blunt-end PCR products. The cycling profile consisted of an initial heating step at 94°C for 5 minutes followed by 35 cycles of denaturation at 94°C for 30 seconds, annealing at 55°C for 45 seconds and extension at 72°C for 1 minute. A final extension at 72°C for 5 minutes concluded the PCR

reaction. PCR was conducted in 0.2 ml thin-walled tubes (Quality Scientific Plastics, CA, USA) in a Perkin Elmer GeneAmp PCR system 2400 (PE Applied Biosystems, CA, USA).

2.2.2.2 Agarose gel electrophoresis of PCR products

All PCR products were analysed on a 1% (w/v) agarose gel (Promega Corporation, Madison, USA) made up in TBE (0.098 M Tris base, 0.098 M boric acid, 2 mM EDTA pH 8.0) or TAE (0.04 M Tris-Acetate, 1 mM EDTA, pH 8.0) containing ethidium bromide added to the gels at <50°C before pouring at a final concentration of 0.4 µg/ml. Electrophoresis was carried out at 70-100 Volts in a minicell EC370M electrophoresis system (E-C Apparatus Corporation, USA) in 1×TBE or TAE buffer. DNA samples were loaded with 10 µl Gel Loading Solution (containing 0.25% w/v bromphenol blue, 0.25% w/v xylene cyanole FF, 40% w/v sucrose; Sigma-Aldrich, USA). 1 µg of a 1 Kb Plus DNA Ladder™ (Life Technologies, USA) was loaded in a separate line for size comparison. DNA fragments were visualised on a UV transilluminator (UVP Inc., CA, USA) and photographed with a Polaroid direct screen instant camera (shutter speed of 1 second), or on a TC-312A 312nm UV transilluminator (Spectroline Corporation, NY, USA) and visualised with a CCD camera (Kodak Digital Systems, NY, USA) linked to a computer system.

2.2.2.3 Gel extraction of PCR 1 products

Each half of the mutated PfHT1 construct was excised with a clean scalpel from a 1% (w/v) agarose/ TBE gel stained with ethidium bromide whilst being visualised on a UV transilluminator. Exposure to the UV was kept to a minimum whenever possible to limit damage of the DNA sustained by UV exposure (e.g. formation of thymine-dimers; Adams *et al*, 1992). Each gel slice was weighed in a 1.9 ml microfuge tube. The QIAquick Gel Extraction Kit (Qiagen Ltd, West Sussex, UK) was used according to the manufacturers instructions. Three volumes of Buffer QG (containing guanidine thiocyanate and pH indicator: yellow at pH ≤7.5, violet at pH >7.5) was added to one volume of gel (100 mg ≈ 100 µl) and incubated at 50°C and vortexed every 2-3 minutes until the gel was dissolved. Once the gel slice was dissolved the colour of the

mixture was checked for the correct pH (≤ 7.5) for maximum absorption on the silica-gel membrane. If the mixture indicated a high pH, 3 M sodium acetate at pH 5.0 was added. The mixture was pipetted into a QIAquick spin column with a 2 ml collection tube and centrifuged for 1 minute at 13000 rpm. The DNA bound to the silica-gel membrane was washed with Buffer QG to remove all traces of agarose and then with Buffer PE (containing ethanol) and centrifuged for 1 minute at 13000 rpm at a time. All trace of Buffer PE was removed by an additional centrifugation step for 1 minute at 13000 rpm. DNA was eluted with Buffer EB (10 mM Tris-Cl, pH 8.5) in a clean 1.9 ml microfuge tube.

2.2.2.4 PCR 2: to obtain the full-length mutants

Both halves of each mutated construct isolated from the agarose gel by the QIAquick gel extraction kit were used as template in two subsequent PCR reactions to extend the full-length gene. The optimal reaction conditions were the same as those indicated in Table 2.4 with HTKB1 and HTKB2 as forward and reverse primers respectively. The gel isolated PCR 1 products were used as template with 0.5 µl of each per reaction. Thermocycling consisted of an initial 5 minute denaturation at 94°C followed by 5 cycles of denaturation at 94°C for 30 seconds, an annealing temperature of 55°C for 90 seconds, and extension at 72°C for 4 minutes to allow for full extension of each half at its 3'end. Before the start of the sixth cycle, primers HTKB1 and HTKB2 were added. Annealing temperature was increased to 60 °C to facilitate higher specificity of priming, otherwise the cycling parameters were the same as for PCR 1.

The number of required cycles after addition of primers had to be optimised. To achieve this, aliquots of 12.5 µl were removed from a 50 µl reaction after 15, 20 and 25 cycles of a 30-cycle reaction. Subsequent reactions were carried out for 15 cycles after addition of primers and the extension time of the last cycle was increased to 8 minutes to accommodate the full 1.5 Kb expected product length. PCR 2 products were isolated from 1% (w/v) agarose gels using the QIAquick Gel Extraction kit as described in Paragraph 2.2.2.3 and concentration of each mutant construct was determined by comparison on an ethidium bromide stained gel with a band from the 1

Kb Plus DNA ladder of known concentration. The pmols of each mutant construct were calculated.

2.2.3 Cloning strategies

2.2.3.1 *Phosphorylation of the 5'-ends of the PCR 2 products*

For the insert to be ligated to the vector by T4 DNA Ligase, the 5'-ends of the PCR 2 product had to be phosphorylated. This was achieved by the Ready-To-Go T4 Polynucleotide Kinase (PNK) kit (Amersham Pharmacia Biotech, London, UK), where the gamma-phosphate of ATP was transferred to a 5'-OH of the PCR 2 products. The Ready-To-Go T4 PNK contains in 50 µl 8-10 units of FPLCpure T4 Polynucleotide Kinase, 50 mM Tris-HCL (pH 7.6), 10 mM $MgCl_2$, 5 mM DTT, 0.1 mM spermidine, 0.1 mM EDTA (pH 8.0), 0.2 µM ATP and stabilizers. It is recommended by the product protocol to add 5-10 pmols of 5'ends of oligonucleotide, but due to a low yield of PCR 2 product after gel extraction only <1 pmol of each could be added. This mixture was incubated at 37°C for 30 minutes. The reaction was stopped by the addition of 5 µl of 250 mM EDTA.

Resulting product was cleaned through the QIAquick PCR purification kit (Qiagen, UK) according to the manufacturer's instructions. This involved adding five volumes of Buffer PB to one volume of the final T4 PNK reaction, and pipetted into a QIAquick spin column contained in a 2 ml collection tube. This was spun for 1 minute at 13000 rpm and then washed with Buffer PE and eluted in 30 µl Buffer EB. Assuming a 100% recovery of the DNA from the columns, a rough estimate was made of the pmols of each sample available for ligation into the pUC18 vector.

2.2.3.2 *Cloning into SmaI cut pUC18 vector*

Three vector-to-insert ratios (measured in pmols) were utilised to determine which ligation ratio would produce the most colonies after transformation. The vector to insert ratios decided on were 1:0.5, 1:1 and 1:3 with the pUC18 vector at 0.056 pmols per ligation reaction. The Ready-To-Go pUC18 *SmaI*/ BAP + Ligase kit (Amersham

Phamacia Biotech, London, UK) was utilised for ligation of the phosphorylated PCR 2 products into *Sma*I cut pUC18 vector that was already dephosphorylated. The manufacturer's instructions were followed and involved adding the DNA and reactants to a final volume of 20 µl and incubating for 3-5 minutes at room temperature. In 20 µl the kit contains 100 ng of pUC18 *Sma*I/ BAP and a minimum of 6 Weiss units of FPLCpure T4 DNA Ligase, 66 mM Tris-HCl (pH 7.6), 6.6 mM $MgCl_2$, 0.1 mM ATP, 0.1 mM spermidine, 10 mM DTT and stabilisers (0.01 Weiss units will ligate 1 µg of DNA in 20 minutes). After the initial incubation at room temperature, the mixture was pipetted and centrifuged to create a homogenous solution and then incubated at 16°C for 30-45 minutes. No heat inactivation of the reaction was necessary.

2.2.3.3 *Transformation of competent cells*

The pUC18 vector-containing insert was transformed into *Epicurian Coli* XL2-Blue Ultracompetent Cells (Stratagene, USA) according to the manufacturer's instructions. The ultracompetent cells were thawed on ice and then aliquoted into prechilled 15 ml Falcon 2059 polypropylene tubes (Strategene, USA). To this β-mercaptoethanol was added to a final concentration of 25 mM. The cells were incubated on ice for 10 minutes while being gently stirred. 2 µl of the ligation reaction from paragraph 2.2.3.2 was added and incubated on ice for a further 30 minutes. The pUC18 plasmid (10 pg) was used as a positive control. The tubes were pulse heated at 45°C for 30 seconds and incubated on ice for 2 minutes. 900 µl of preheated (42°C) NZY^+ broth (1% w/v NZ amine, 0.5% w/v yeast extract, 0.5% w/v NaCl, 12.5 mM $MgCl_2$, 12.5 mM $MgSO_4$, 20 mM glucose, NaOH to pH 7.5) was added and the tubes incubated at 37°C for 1 hour while shaking at 225-250 rpm. 100 µl of each reaction was plated on LB broth plates (1% w/v tryptone, 0.5% w/v yeast extract, 1% w/v NaCl, 1.5% w/v agar, 100 µg/ml ampicillin). Since the pUC18 vector contains the LacZ gene there was also the option of blue/ white selection and therefore the plates were first prepared with 40 µl of 2% w/v X-gal (LacZ gene encoded protein substrate) and 4 µl of 1 mM IPTG (LacZ gene activator).

2.2.4 Plasmid isolation

2.2.4.1 *Conventional miniprep plasmid isolation*

White colonies were selected off plates produced from the transformation reaction mentioned in Paragraph 2.2.3.3 and a preliminary screening of these colonies for the presence of an insert was carried out using an alkaline lysis protocol (Sambrook *et al*, 1989). Five white colonies were selected off each plate (S302A and L304T) and grown up in 3ml LB broth containing 50 µg/ml ampicillin. 1 ml of each was aliquoted into a 1.9 ml microfuge tube and centrifuged at 13000 rpm for 1 minute. The pellet was resuspended in 100 µl Solution 1 (50 mM glucose, 25 mM Tris-HCl pH 8.0, 10 mM EDTA pH 8.0). Lysis of the bacteria was induced by addition of 100 µl Solution 2 (1% w/v SDS, 0.2 M NaOH) and incubation at room temperature for no longer than 5 minutes. This lysis was stopped by the addition of 150 µl Solution 3 (3 M potassium acetate, 5 M Acetic acid) followed by incubation for 5 minutes and centrifugation at 13000 rpm for 10 minutes. The plasmid DNA was precipitated with ice-cold 100% ethanol and washed with ice-cold 70% v/v ethanol. The pellet was dissolved in TE buffer (1 mM Tris-HCl pH 8.0, 1 mM EDTA, 2 ug/ml RNase, no incubation required) and resolved on a 1% w/v agarose gel containing 0.4 µg/ml ethidium bromide alongside 1 µg of a 1 Kb Plus DNA Ladder, and visualised over a UV transilluminator.

2.2.4.2 *High pure plasmid isolation*

Of the five colonies selected for each mutant construct, S302A had four positive clones and L304T five positives. All clones that tested positive for correct insert and mutation (Section 2.2.5) were re-grown in LB broth containing ampicillin. The plasmid was isolated using the QIAprep spin miniprep kit (Qiagen Ltd, West Sussex, UK) following the manufacturer's instructions. 3 ml of each culture was pelleted in 1.9 ml microfuge tubes. The pellet was resuspended in Buffer P1 (50 mM Tris-HCl pH 8.0, 10 mM EDTA, 100 µg/ml RNase A). Lysis Buffer P2 (200 mM NaOH, 1% w/v SDS) was added to each sample and incubated at room temperature for no longer than 5 minutes. The Lysis reaction was stopped by addition of chilled Buffer N3 (containing chaotropic salts) with immediate mixing. This was incubated on ice for 5

minutes and then centrifuged for 10 minutes at 13000 rpm. The supernatant was pipetted into a QIAprep spin column with 2 ml collection tube and spun for 1 minute at 13000 rpm. The column was washed with Buffer PE (containing ethanol) and centrifuged twice at 13000 rpm to remove residual buffer. The DNA was eluted off the column with Buffer EB (10 mM Tris-HCl, pH 8.5).

2.2.5 Restriction mapping of recombinant clones

2.2.5.1 Isolation of insert

Plasmids from 5 selected colonies of each mutant were isolated with the conventional method (Paragraph 2.2.4.1) and were digested with *Bgl*II (Life Technologies, London, UK) to release the insert and simultaneously with *Hha*I (Life Technologies, London, UK) to fragment the pUC18 vector. The most suited buffer compatible with both enzymes (REact3, 50 mM Tris-HCl pH 8.0, 10 mM $MgCl_2$, 100 mM NaCl) was added, with 0.3 mg/ml BSA in a 20 µl reaction volume. The reactions were incubated at 37°C overnight. 5 µl of the reaction was run on a 1% w/v agarose gel containing 0.4 µg/ml ethidium bromide alongside a 1 Kb Plus DNA Ladder, and visualised over a UV transilluminator. Inserts required for cloning into the *X. laevis* expression vector pSP64T were extracted with the QIAquick Gel Extraction kit (Paragraph 2.2.2.3).

2.2.5.2 Mapping of mutants

A restriction site had been devised for each mutant over the mutated area during primer design (Paragraph 2.2.1). Mutant S302A was identified by restriction digestion with *Pst*I and mutant L304T by restriction digestion with *Kpn*I (Table 2.2). 4 µl of the digestion mixture described in Paragraph 2.2.5.1 was used in a 10 µl reaction containing each individual enzymes supplied buffer and 0.5 mg/ml BSA. The reactions were incubated at 37°C overnight and were run on a 1% w/v agarose gel containing 0.4 µg/ml ethidium bromide alongside a 1 Kb Plus DNA Ladder, and visualised over a UV transilluminator. Clones that contained the correct mutant insert were frozen in glycerol stocks (15% v/v glycerol) at -70°C.

2.2.6 Expression vector (pSP64T) cloning strategy

2.2.6.1 Cloning into pSP64T

The pSP64T expression vector is described further in Paragraph 3.1. One clone was chosen for each mutant construct S302A and L304T that had been determined to contain the correct mutation by restriction digestion (Paragraph 2.2.5.2). The inserts contained in the pUC18 clone were digested out (Paragraph 2.2.5.1) and isolated from an agarose gel with the QIAquick Gel Extraction kit (Paragraph 2.2.4). Aliquots of the isolated fragments were run on a 1% (w/v) agarose gel and the concentrations were estimated by comparison of a known standard in the 1 Kb DNA Ladder. The final concentration of the *Bgl*II digested, dephosphorylated pSP64T vector was 25 ng/µl. A 2:1 vector to insert molar ratio was used, which by prior ligation reactions was determined to produce the best results. Vector and insert were added to a 1.9 ml microfuge tube together with 1× T4 DNA Ligase buffer and 5 Units of T4 DNA Ligase (Pharmacia Biotech Ltd., UK). The reaction mixture was heated at 45°C for 5 minutes to separate self-attached fragments, followed by incubation at 16°C overnight. The ligation reaction was used directly for transformation into *E. Coli* XL2-Blue Ultracompetent Cells following the strategy described in Paragraph 2.2.3.3.

2.2.6.2 Screening for pSP64T vector containing insert

The transformed cells were plated on LB agar plates (15% w/v agar) containing 100 µg/ml Ampicillin. Clones were picked and grown up in LB broth containing 50 µg/ml Ampicillin. Plasmids were isolated using the conventional plasmid isolation method described in Paragraph 2.2.4.1. All clones that contained insert were linearised with *Xba*I (Life Technologies, London, UK) with incubation at 37°C and visualised on a 1% w/v agarose gel containing ethidium bromide on a UV transilluminator (expected size ≈ 4.7 Kb).

Since there is only one RNA promoter region in the pSP64T expression vector (SP6, Appendix Ia) that can be used for cRNA transcription, the orientation of the insert was checked by digestion with *Hind*III (Life Technologies, London, UK). This was possible because PfHT1 contains only one *Hind*III site within its ORF, which is

200 ng/µl of template was used in each reaction with 3.2 pmols of primer and 2 µl BigDye™ Terminator Cycle Sequencing Ready Reaction Mix (Perkin-Elmer Applied Biosystems, UK) to 5 µl final reaction volume. PCR was performed on a Perkin Elmer GeneAmp PCR system 9700 (PE Applied Biosystems, CA, USA) with 32 cycles of 96°C for 10 seconds, 50°C for 5 seconds and 60°C for 4 minutes. The PCR reaction products were precipitated with 100% ice-cold ethanol at room temperature for 25 minutes, centrifugated at 13000 rpm for 15 minutes and washed with 70% ice cold ethanol. The resulting pellet was dried *in vacuo* and refrigerated at 4°C until use. The sequencing product was analysed on a 36 cm gel in an automated ABI Prism 377 DNA Automatic Sequencer (PE Applied Biosystems, California, USA) and the raw data were analysed with the ABI Prism Sequencing Analysis Version 3.0 software. Sequence alignments were analysed with the ABI Prism Sequencing Navigator Version 1.0.1 software.

2.2.9 Synthesis of cRNA

2.2.9.1 Linearisation and purification of DNA template

Plasmids obtained from the QIAprep spin miniprep kit were linearised with *XbaI* in a 50 µl reaction volume containing appropriate buffer and 0.2 mg/ml BSA with incubation at 37°C overnight. The restriction enzyme was digested by the addition of 7 µg/µl Proteinase K (Macherey-Nagel) in a 1×buffer (10 mM Tris-HCl, 2 mM $CaCl_2$, pH 8.0) and incubation at 50°C for 1 hour. The resulting digest was extracted with an equal volume of phenol/ chloroform and again with an equal volume of chloroform. The organic phase was re-extracted with 50 µl of water. The DNA was precipitated overnight at -20°C with $1/10^{th}$ the volume of 3 M NaAc and 2.5× the volume of 100% ethanol. The precipitate was collected by centrifugation at 13000 rpm for 20 minutes and then washed with 70% ethanol. The dried pellet was dissolved in filtered, DEPC treated water (0.1% diethyl pyrocarbonate in double glass-distilled, deionised H_2O, with removal of DEPC by autoclaving). The resulting DNA was quantified using a fluorometer (Paragraph 2.2.7).

2.2.9.2 *Transcription reaction*

Transcription of cRNA was achieved with the use of two separate kits. The initial kit used was the mMESSAGE mMACHINE™ (Ambion, UK) SP6 kit. 1 µg of the purified DNA template was added together in a 20 µl reaction volume with 1× Transcription Buffer (patent protected, contains salts, buffer, dithiothreitol and other ingredients), 1× Ribonucleotide Mix (5 mM ATP, CTP, UTP; 1 mM GTP and 4 mM Cap Analogue), 1× Enzyme Mix (SP6 RNA polymerase, ribonuclease inhibitor, buffer, 50% glycerol buffer), and the volume adjusted with the supplied RNase-free water. The reaction was incubated at 37°C for 3 hours, after which 2 units of the supplied RNase-free DNase I was added and the mixture was further incubated at 37°C for 15 minutes. The reaction was terminated and the RNA recovered by the addition of nuclease-free water and the supplied Lithium Chloride Precipitation Solution (7.5 mM lithium chloride, 75 mM EDTA). This was incubated at -20°C overnight and then centrifuged at 13000 rpm for 30 minutes at 4°C. The pellet was washed in nuclease-free 70% ethanol and dried at room temperature. The dried pellet was dissolved in nuclease-free water on ice, and aliquoted into nuclease-free tubes with 1µl per tube and frozen at -70°C.

Alternatively, cRNA was synthesised with the SP6 Cap-Scribe kit (Boehringer Mannheim, Germany). The transcription reaction was set up with 1,5 µg of linearised clean DNA template together with 1× Cap-Scribe buffer, 40 units of SP6 RNA polymerase and nuclease-free water to a volume of 20 µl. This reaction mixture was incubated at 37°C for 3 hours after which 2 units RNase-free DNase I (Promega Corporation, Madison, USA) was added and incubated for a further 30 minutes at 37°C. The reaction was stopped by the addition of 15 µl of ammonium acetate stop solution (5 M ammonium acetate, 0.1 M EDTA) and 115 µl of filtered, DEPC treated water. The mixture was extracted with an equal volume of RNase-free phenol/chloroform and again with RNase-free chloroform. This aqueous phase (≈ 200 µl) was filtered through a Milex-GV 0.2 µm filter (Millipore, USA) to remove any contaminating salts. The cRNA was pelleted by the addition of isopropyl alcohol and an incubation at -20°C overnight followed by centrifugation at 13000 rpm for 30 minutes at 4°C. The pellet was washed in nuclease-free 70% ethanol and dried at

room temperature. The dried pellet was dissolved in DEPC-treated, filtered water on ice and aliquoted into nuclease-free tubes with 1 µl per tube, which were frozen at -70°C.

2.2.10 cRNA quantification

The presence of cRNA was confirmed by running an aliquot of the transcription reaction on an agarose gel. A mixture containing 1 µl cRNA, 0.07 µg/µl ethidium bromide and RNA loading buffer (80% formamide, 0.1% xylene cyanol, 0.1% bromophenol blue, 2 mM EDTA) was heated at 70°C for 2 minutes and then snap-cooled on ice. This was run on a 1% w/v agarose gel together with 0.24-9.5 Kb RNA Ladder (Life Technologies, UK). The cRNA was visualised on a transilluminator and photographed with a Polaroid direct screen instant camera.

The concentration of the cRNA was determined on a Shimadzu UV 160 A spectrophotometer. 1 µl of synthesised cRNA was diluted to 300 µl with DEPC treated water. The spectrophotometer was blanked with DEPC-treated water and the absorbancy was read at 260 nm. The cRNA concentration in µg/ml was calculated with the following equation (Sambrook *et al*, 1989):

$$A_{260} \times \text{dilution factor} \times 40 = \mu g/ml$$

2.3 Results

2.3.1 Primer design

Primers AGT1&2 produced a double point mutated construct (302SGL→AGT) of amino acid S302 and L304. Primers AGL1&2 and primers SGT1&2 produced single point mutated constructs S302A and L304T, respectively. All three sets of the complementary primers contained restriction sites designed to lie directly or close to the mutated site (Figure 2.2). All possible restriction sites not present in the wild type were modelled over the mutated regions to identify sites for reconstruction without any amino acid changes. This would produce a unique restriction site that would only

be cut if the mutation was present and would enable rapid screening of viable clones without sequencing.

```
Wild-type: 892 GGA TGT TTG TTA TCT GGT TTA CAA CAA TTT ACA GG
Amino Acid 298 Gly Cys Leu Leu Ser Gly Leu Gln Gln Phe Thr
Target Motif:              302 S   G   L
AGT mutant:892 GGA TGT TTG TTA GCT GGT ACA CAA CAA TTT ACA GG
Mutated Motif:             302 A   G   T
Primer AGT1:   GGA TGT TTG CTA GCT GGT ACA CAA CAA TTT ACA GG
```

Figure 2.2: Primer AGT1 is used here to demonstrate how a restriction site could be modelled over or near a mutated area. The restriction site *Nhe*I used in this example is underlined. Mutated amino acids are indicated in bold.

2.3.2 PCR reaction

For each new mutation, two PCR 1 reactions were carried out to create each half of the mutated construct. For example, for construct S302A, primers HTKB1and AGL2 were used in one reaction with primers AGL1 and HTKB2 in a second separate reaction (Figure 2.3).

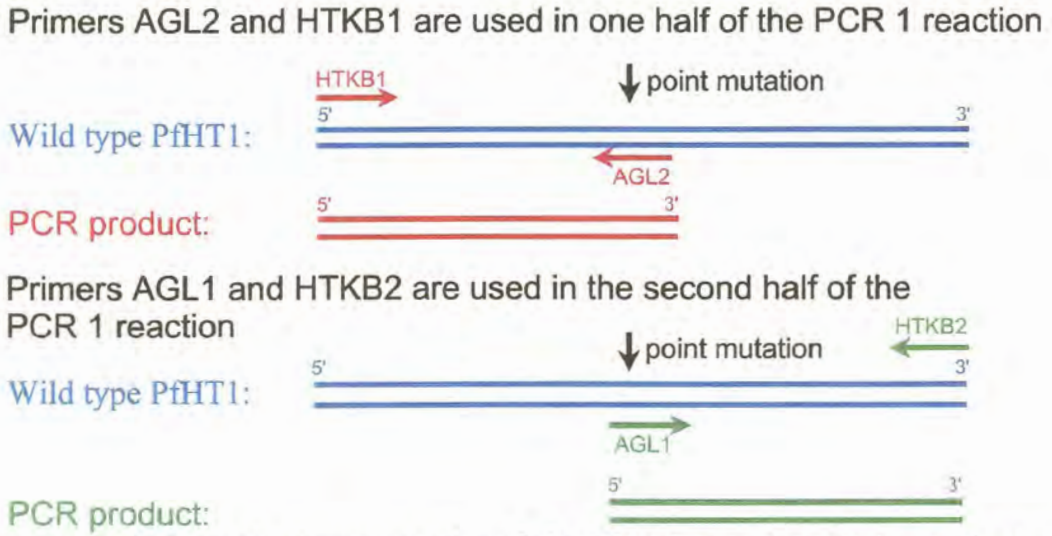

Figure 2.3: Schematic demonstration of the PCR 1 reaction. Each set of primers indicated together are included in two separate PCR reactions of 25 µl each according to the conditions set in Table 2.4.

Primers AGL1&2 and SGT1&2 with HTKB1&2 proved successful at a 55°C annealing temperature, which is 10-20°C lower than their calculated Tm's. As shown

in Figure 2.4, primers HTKB1 with AGL2 and HTKB1 with SGL2 when visualised on an agarose gel produced bands of size 0.9 Kb. Primers AGL1 with HTKB2 and SGL1 with HTKB2 when visualised on an agarose gel had produced bands of size 0.6 Kb. These bands were isolated from the agarose gels and used as template in the PCR 2 reaction (Figure 2.5).

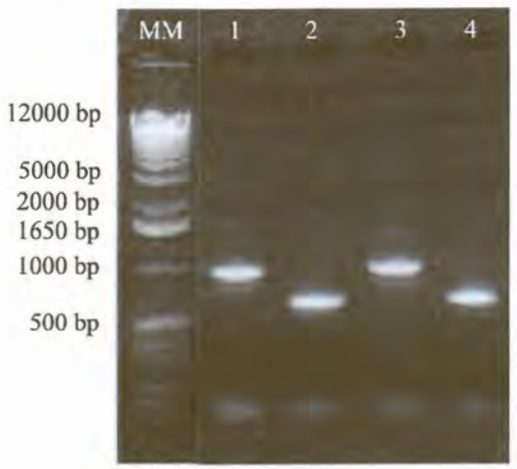

Figure 2.4: Results of the PCR 1 reaction. This PCR reaction produced the mutated motifs and the bands indicate the two halves of the full-length gene. MM indicates the 1 Kb Plus DNA Ladder. Lane1 contains product produced from primers HTKB1 and AGL2. Lane2 contains product produced from primers AGL1 and HTKB2. Lane3 contains product produced from primers HTKB1 and SGL2. Lane4 contains product produced from primers SGL1 and HTKB2.

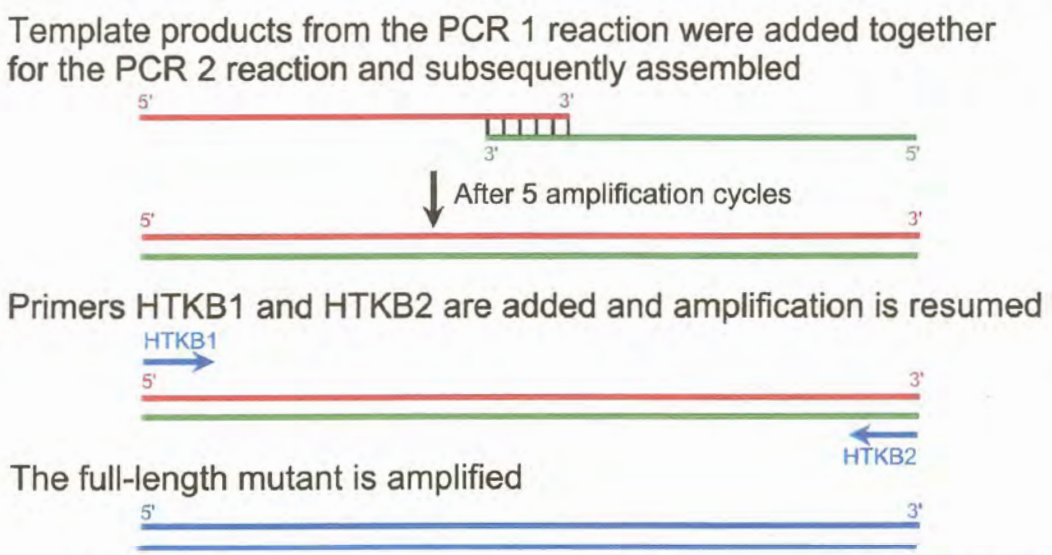

Figure 2.5: Schematic demonstration of the PCR 2 reaction with HTKB1 and 2 as primers with PCR 1 product as template.

PCR 2 proved more difficult and a few reaction parameters were varied to determine the optimum reaction conditions. Those varied were the magnesium concentration

(results not shown), the template concentration (Figure 2.6A), the annealing temperature (results not shown) and the number of cycles (Figure 2.6B). To determine the optimum number of cycles with a 1:10 dilution, a reaction volume of 50 µl was used and 12.5 µl was removed from the reaction mix after 15, 20 and 25 cycles.

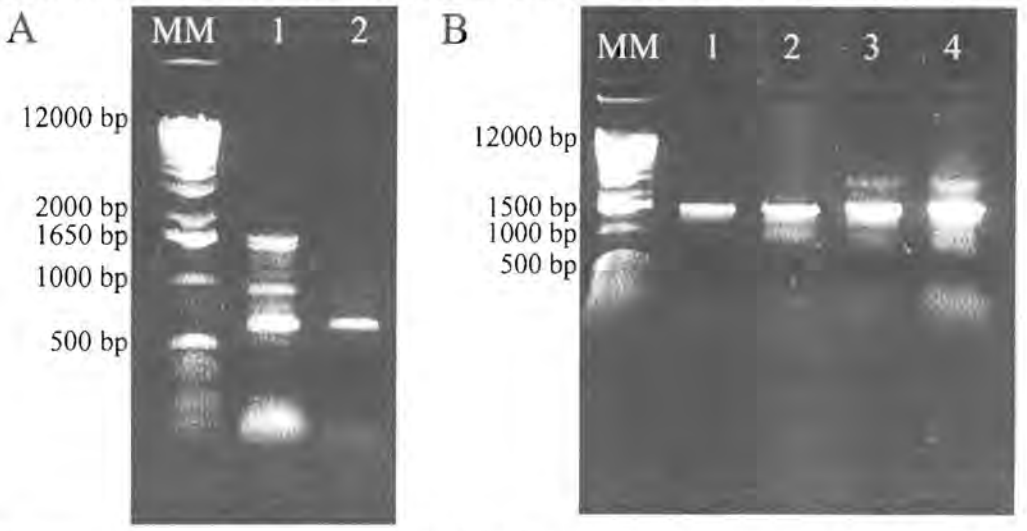

Figure 2.6: Optimisation of the PCR 2 reaction. MM in both A and B indicates the 1 Kb Plus DNA Ladder. **Figure A** represents the template concentration optimisation. Lane 1 indicates the results obtained from a 1:10 dilution and Lane 2 indicates a 1:100 dilution of the PCR 1 column cleaned templates, both amplified for 30 cycles. The expected band size is ≈ 1500 bp. **Figure B** shows product from differing number of cycles with a 1:10 dilution and gel extracted PCR 1 product as template. Lanes 1, 2, 3 and 4 are an indication of product produced after 15, 20, 25 and 30 cycles respectively.

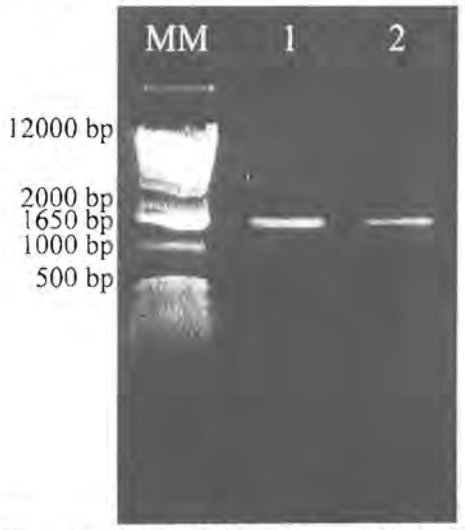

Figure 2.7: Full-length amplification of the mutated constructs. MM indicates the lane containing the 1 Kb Plus DNA Ladder. PCR 2 was conducted with 15 amplification cycles, and a 1:10 dilution of gel extracted PCR 1 product. The concentration of each mutant construct was estimated by comparison of the 100 ng 1650 bp band. Lane 1 represents 80 ng/ 5µl (16 ng) of AGL mutant construct. Lane 2 represents 40 ng/ 5µl (8 ng) of SGT mutant construct.

The PCR 1 template mixtures were first purified through a PCR Purification column (Qiagen, UK) before being used as template for PCR 2 and the outcome of the PCR 2 reaction showed multiple bands indicating either non-specific priming or over amplification (Figure 2.6A). Extracting the PCR 1 product from a gel before being used in PCR 2, and reducing the number of cycles eliminated these bands (Figure 2.6B, Lane 1). From the optimisation reactions, a 15-cycle reaction was decided on with a 1:10 dilution. Products from PCR 2 were visualised as shown in Figure 2.7.

2.3.3 Selection of correct constructs in pUC18 vector

For each mutant construct five colonies that appeared white, that resulted from the transformation into pUC18 vector, were selected from the agar plates. As shown in Figure 2.8 four out of the five colonies selected for mutant AGL produced plasmid containing an insert and all five colonies selected for mutant SGT had plasmids with inserts (expected band size ± 4.5 Kb). Plasmids the same size as the pUC18 vector used as a negative control indicated no insert present.

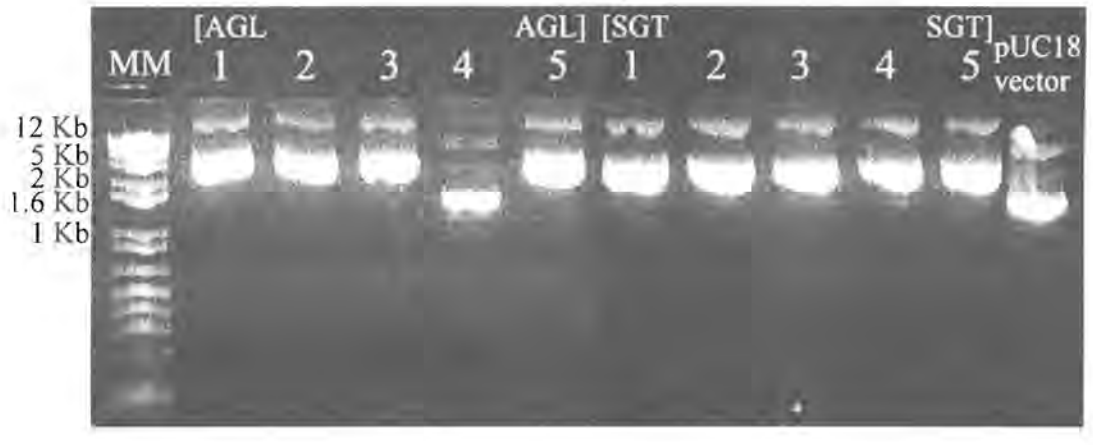

Figure 2.8: Confirmation of the presence of insert for colonies selected. The resulting plasmid isolated from five colonies selected for the AGL mutant construct and from five colonies selected for the SGT mutant construct. The pUC18 vector was used for size comparison. MM represents the 1 Kb Plus DNA Ladder.

Plasmids isolated from colonies selected for each construct were digested with restriction enzymes *Bgl*II to isolate the insert. The plasmids were also simultaneously digested with *Hha*I, which due to the many *Hha*I site in the pUC18 vector digests the

pUC18 vector into fragments smaller than 350 bp. Figure 2.9A shows the insert at 1.5 Kb. The absence of a band at this size indicates no insert in the clone. The resulting digest shown in Figure 2.9A was re-digested with the appropriate restriction enzymes to establish the presence of the mutated motif. Figure 2.9B shows the results obtained from this digest. Figure 2.9B, Lanes 1-4 show almost complete digestion of the AGL mutant construct with *Pst*I resulting in two bands of 1 Kb and 500 bp and a faint band at 1.5 Kb. Figure 2.9B, Lanes 5-9 show an incomplete digestion of the SGT mutant construct with *Kpn*I resulting in three bands of 1.5 Kb, 1 Kb and 500 bp.

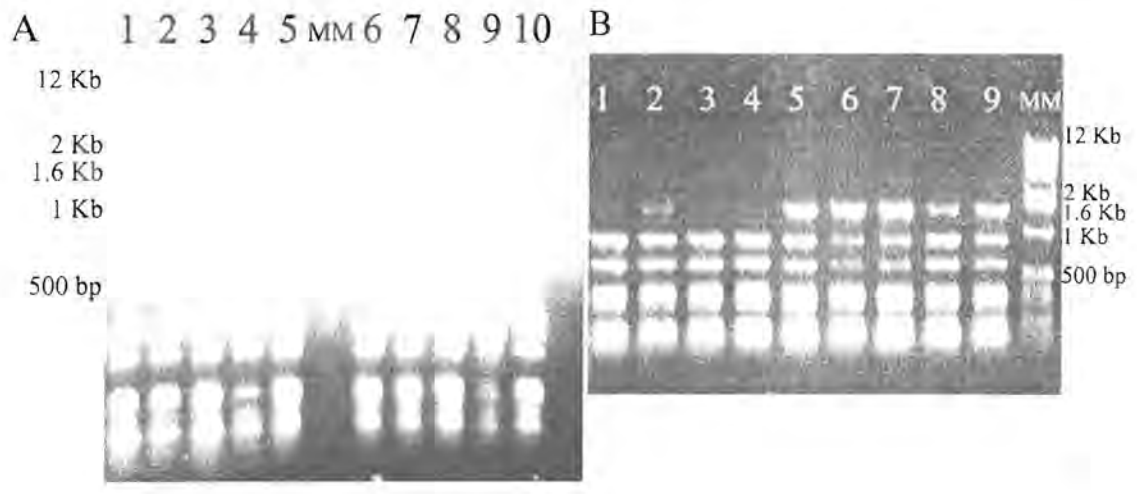

Figure 2.9: Confirmation of insert by restriction enzyme digestion. Figure A indicates the results obtained by digestion with restriction enzyme *Bgl*II and *Hha*I. Lane 1-5 represents insert from plasmids obtained from the AGL construct. Lane 4 clearly indicates the absence of insert. Lane 5-10 represents insert from plasmids obtained from the SGT construct. **Figure B** Lanes 1-4 indicates AGL construct digested with *Pst*I. Lanes 5-9 indicates SGT construct digested with *Kpn*I. MM represents the 1 Kb Plus DNA Ladder.

2.3.4 Gel extraction

Figure 2.10A shows the AGL and SGT *Bgl*II digested inserts as 1.5 Kb bands before gel extraction, and Figure 2.10B shows the resulting product after gel extraction. Also present in Figure 2.10B is a band of approximately 3 Kb, which persisted even after careful gel extraction of the band shown in Figure 2.10A.

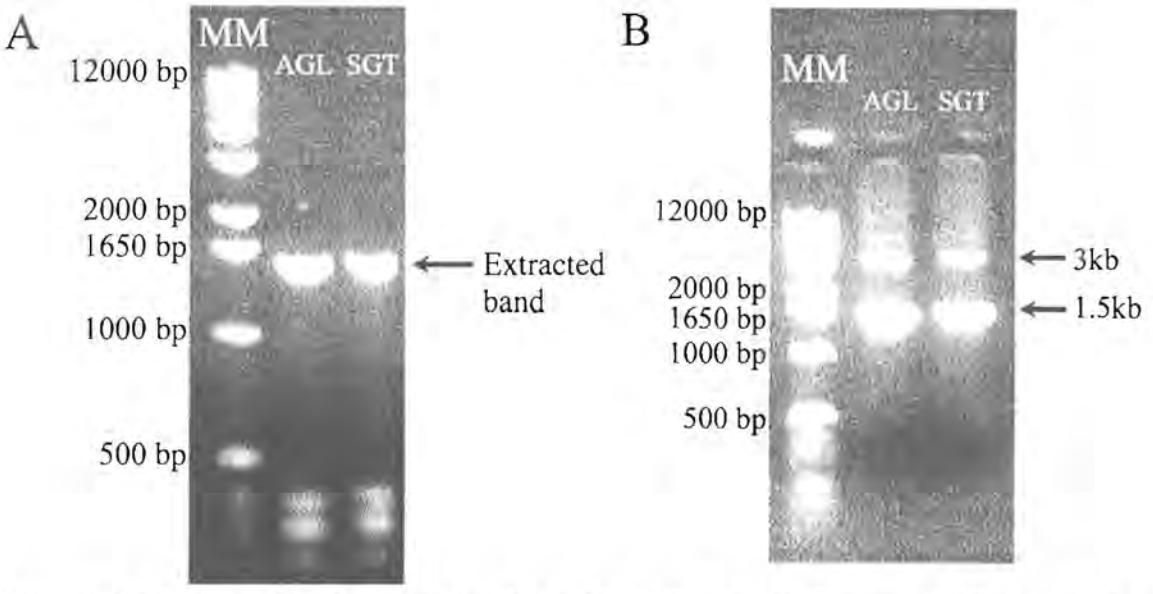

Figure 2.10: Results of gel extraction of *Bgl*II cut AGL and SGT mutant constructs. Figure A indicates the 1.5Kb insert resulting from the simultaneous digestion with *Bgl*II and *Hha*I before being extracted from the gel. **Figure B** is the resulting gel extracted product. MM represents the 1 Kb Plus DNA Ladder.

2.3.5 Selection of correct insert from pSP64T

After insertion of insert shown in Figure 2.10B into pSP64T expression vector, the vector was cloned into competent *E. coli* cells. Since no blue/white selection of colonies was possible, all resulting colonies were picked from agar plates and inoculated into LB broth containing ampicillin. 16 colonies were grown up for the AGL mutant, and 17 were grown up for the SGT mutant. Of the 16 colonies from the mutant AGL construct, 11 produced plasmid that contained insert. Of the 17 colonies from mutant SGT construct, 11 produced plasmid that contained insert. The presence of the insert in those plasmids that appeared to contain them was confirmed by linearisation.

All plasmids were digested with *Hind*III to determine the orientation of the insert. Of the 11 plasmids containing the AGL mutant construct, 4 were in the correct orientation indicated by the presence of a 1.2 Kb and 3.5 Kb band (Figure 2.11). Of the 11 plasmids containing the SGT mutant construct, 2 were in the correct orientation. All those that produced a band of 400 bp and a band of 4.3Kb were in the incorrect orientation.

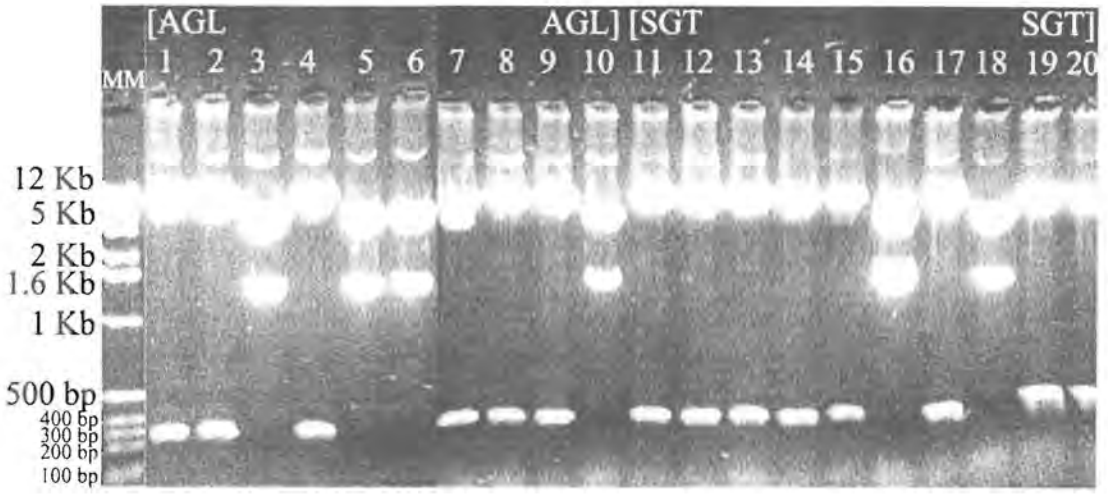

Figure 2.11: Evaluation of the correct orientation of insert in the pSP64T vector. Lanes 1-20 represent plasmids digested with *Hind*III to determine their orientation. Lanes 3, 5, 6 and 10 show plasmids from the AGL mutant containing an insert of the correct orientation. Lane 16 and 18 show plasmids from the SGT mutant containing an insert with a correct orientation. MM represents the 1 Kb Plus DNA Ladder.

2.3.6 Sequencing

The AGL and SGT mutant constructs contained in the pSP64T expression vector were sequenced before being used for cRNA transcription. The results from the analysis of the sequencing reaction over the mutated area confirmed the presences of the AGT mutant motif and the SGT mutant motif. These clones were renamed XA1.4 and XT1.10 respectively.

2.3.7 Transcription of cRNA

In order to commence cRNA transcription, the DNA template first needed to be linearised and cleaned to remove contaminating proteins and salts from the restriction digest. Figure 2.12A demonstrates DNA quality and yield after restriction enzyme digestion before and after Proteinase K digestion and phenol/chloroform extraction on a 1% w/v agarose gel. The resulting cRNA is shown in Figure 2.12B next to a 0.24-9.5 Kb RNA Ladder. The expected band size of the cRNA was approximately 1.5 Kb.

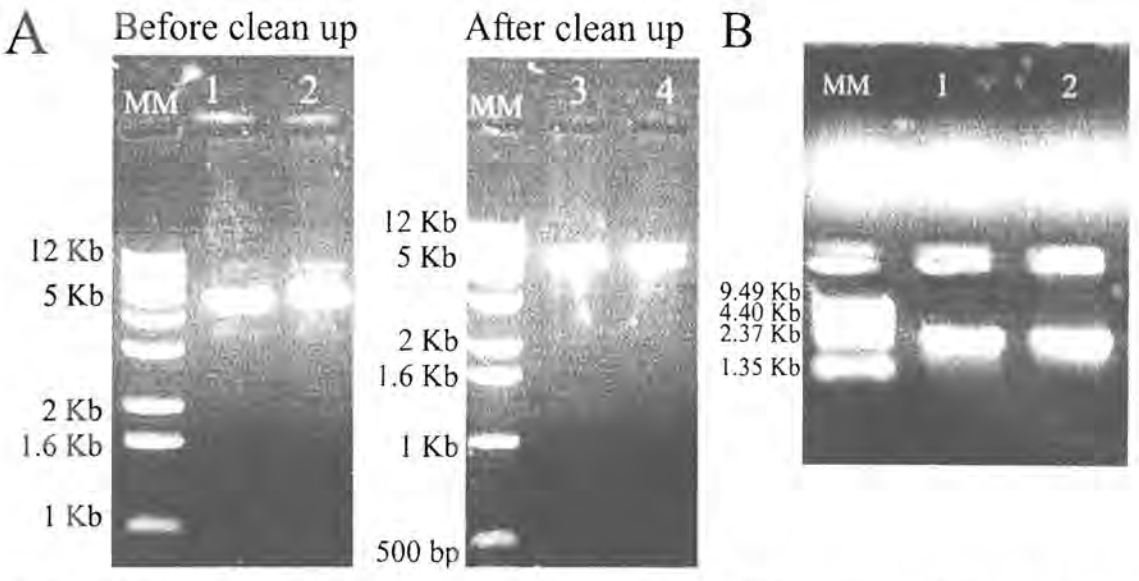

Figure 2.12: cRNA transcription DNA template and transcription product. **Figure A** shows the DNA template that was used in the cRNA transcription reaction. Lanes 1 and 2 represents the DNA template before clean-up and Lanes 3 and 4 represent the DNA template after clean-up. MM represents the 1 Kb Plus DNA Ladder. **Figure B** demonstrates the resulting cRNA from the transcription reaction on a non-denaturing agarose gel. MM represents the 0.24-9.5 Kb RNA Ladder.

The yield of cRNA after quantification with the spectrophotometer varied between 2.5 µg/µl and 5 µg/µl after being dissolved in 7-10 µl nuclease-free water. This was equivalent to a total yield of cRNA between 17.5 µg and 35 µg for every 1-1.5 µg DNA template and was close to the manufacturers predicted yield after proper use of the kit. From the spectrophotometric analysis of the cRNA, it was also observed to contain no protein or high salt contamination.

2.4 Discussion

Considering the importance of the *P. falciparum* glucose transporter PfHT1 and the role it could play in anti-malarial chemotherapy, the need for more information on this transporter is vital. Without the availability of the crystal structure of this transporter, mutational studies are presently one method to obtain structure-function information. Thus far studies on PfHT1 have revealed that it is a hexose transporter capable of transporting D-glucose and D-fructose with K_m values of 1.0 ± 0.2 mM and 11.5 ± 1.6 mM, respectively. The endofacial ligand Cytochalasin B shows high affinity for PfHT1 ($K_i \approx$ 1.4-4.3 µM) and the exofacial binding site probe 4,6-*O*-ethylidene-α-D-

glucose shows poor affinity for PfHT1 (K_i > 50 mM). Mutational studies have shown that the conserved residue Q169 in helix 5 mutated to asparagine results in the ablation of fructose transport (Woodrow *et al*, 2000).

Previous studies on the GLUT1 transporter have established a possible role for helix 7 in fructose/ glucose transport and helix 7 has also been implicated in exofacial ligand binding (Seatter *et al*, 1998). Most literature concerning helix 7 has focused on the QLS motif that is conserved within glucose transporters (GLUT1, 3 and 4) but is not present in hexose (GLUT2) or fructose (GLUT5) transporters (Table 2.1). Studies by Seatter *et al* (1998) suggested that the QLS motif confer on the transporter the ability to transport glucose at a higher affinity than the transporter would have if this motif were absent. This QLS motif in GLUT1 corresponds to a SGL motif in PfHT1. Mutation of PfHT1 helix 7 SGL motif to GLUT1 QLS resulted in no detectable uptake of either glucose or fructose (S. Krishna, unpublished results), which could be either due to a dysfunctional transporter or interrupted trafficking of the transporter to the oocyte membrane. The corresponding motif of *T. brucei* hexose transporter THT1 is an AGT motif. The affinity of THT1 for glucose is comparable to that of PfHT1, whilst its affinity for fructose is higher (K_i = 2.56 ± 0.40 mM; Tetaud *et al*, 1997) than that of PfHT1 (K_i ≈ 11.15 mM; Woodrow *et al*, 2000). Therefore the AGT motif in *T. brucei* was substituted for the SGL motif in PfHT1 in order to determine its role in glucose/ fructose binding. If this motif is responsible for fructose transport, its substitution is expected to increase the transporters ability to transport fructose. Binding of glucose to this motif can also be investigated with glucose analogues (explored in Chapter 3).

Primers were designed to incorporate mutations within the SGL motif of PfHT1. Primers of approximately 35 bases were designed to produce an SGL→AGT mutant. The length of the primers differed from the conventional length of primers of approximately 24 bases since base changes within the primer often results in lower stringency. Where bases between the primer and template are no longer complementary, binding becomes unstable at high annealing temperatures resulting in primer detachment from the template and reduced product. In this case the longer primers had a larger complementary area at the 3' end for stable priming. Additional

mutations within the helix 7 SGL motif included mutations of only one of the amino acids at a time within the motif to produce two mutants S302A and L304T intended to identify the amino acid within the motif responsible for any deviations in substrate-protein interaction (Table 2.2).

Restriction sites were included near the mutated motif. Even though primer design was limited, the primers were highly successful in the PCR 1 reactions and provided little difficulty (Figure 2.4). This was not the case for the PCR 2 reaction. Only after gel extraction of the PCR 1 products used as template for PCR 2 and optimisation of the PCR 2 reaction could the full-length gene product be recovered. For optimisation of the PCR 2 reaction, different dilutions of the template obtained from the first reaction were tested (Figure 2.6A). In Figure 2.6A, 1:10 and 1:100 dilutions of column purified PCR 1 product, which are then amplified in PCR 2, are shown. Figure 2.6A shows that a higher dilution (1:100) produces less non-specific amplification bands, but the expected band size of ≈ 1500 bp is only faintly visible. Thereafter the PCR 1 products were purified by gel extraction and used as a 1:10 dilution for PCR 2. The annealing temperature was raised to 60°C, which reduced the non-specific bands. The number of cycles used per reaction was optimised (Figure 2.6B). As shown in Figure 2.6B, excessive amplification cycles produced more non-specific amplified bands. Therefore a program of 15 cycles was decided on with a 1:10 dilution of template and an annealing temperature of 60°C.

Mutated clones in the pUC18 vector were checked for the presence of the correct mutation by restriction enzyme digestion in order to limit the number of clones to be sequenced. Partial digests of the AGL and SGT mutants are shown in Figure 2.9B. Since digestion of the inserts did occur, the presence of the mutations within the inserts was confirmed. After ligation of the mutated inserts into pSP64T, the presence of the mutated motifs was further confirmed by sequencing. The orientation of the insert in the pSP64T expression vector was determined by the use of restriction enzymes. The different sizes of bands produced by digestion with *Hind*III was used for identification of the correct orientation.

Two cRNA synthesis kits were used for the synthesis of cRNA. The Ambion kit was used at the St. Georges Hospital Medical in London. This kit was designed by a company specialising in RNA related products and the cRNA synthesised from this kit could be directly used for *in vivo* translation. The synthesis of cRNA was accomplished at the University of Pretoria using the Roche SP6 Cap Scribe. This kit did not specify that the cRNA produced could be directly used for *in vivo* translation and was specific for use in *in vitro* work. However the kit still produced cRNA in amounts equivalent to those produced by the Ambion kit and this cRNA was then was used for *in vivo* translation. The cRNA produced (Figure 2.12B) was used for microinjections into *Xenopus laevis* oocytes. The effects of the above produced mutants on glucose transport were determined by kinetic analysis in comparison to the wild type and presented in Chapter 3. In addition to these helix 7 mutants, a helix 5 mutant (Q169N) mentioned in Chapter 2.1 was also explored kinetically. This mutation resulted in the ablation of fructose transport (Woodrow *et al*, 2000).

3 CHAPTER THREE:

EXPRESSION AND KINETIC ANALYSIS OF THE PFHT1 HEXOSE TRANSPORTER IN *XENOPUS LAEVIS* OOCYTES

3.1 Introduction

The *Xenopus laevis* oocyte expression system was first used for the expression of rabbit reticulocyte 9S mRNA in 1971 and has since led to the expression of a variety of proteins. Apart from soluble proteins, the system has also been used for the expression of receptors, channel proteins and transporters (Hediger *et al*, 1987). The oocytes are ideal for expression of eukaryotic proteins since the synthesised proteins are subjected to post translational modifications such as glycosylation and are usually correctly folded and inserted into the cell membrane (Yao *et al*, 2000). Applications of the *X. laevis* expression system are shown in Figure 3.1.

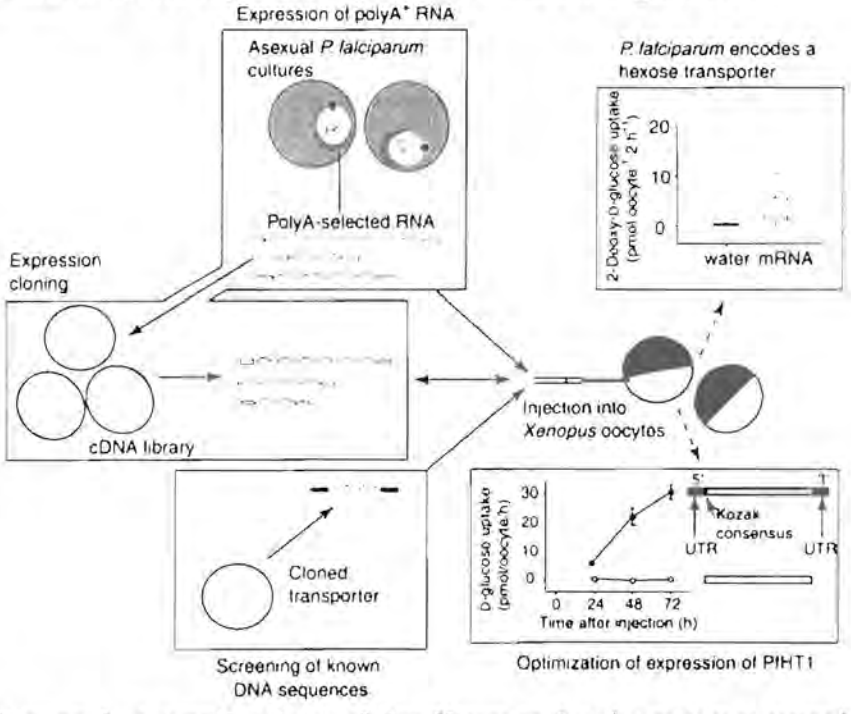

Figure 3.1: Applications of the *Xenopus laevis* oocyte expression system. *In vitro* transcribed cRNA of genomic DNA from cultured *P. falciparum*, cDNA libraries or clones are injected into *Xenopus* oocytes to reveal the possible functions and properties of translated proteins (Krishna *et al*, 2000).

The *X. laevis* frog is indigenous to South Africa, Botswana and South West Zimbabwe. The frogs are members of the family *Pipidae* and can be identified by having three claws on both their hind limbs (Figure 3.2A). For oocyte expression experiments female frogs are used and can be distinguished from males by their larger size and more prominent cloacal valves (Smart and Krishek, 1995). The oocytes are obtained from wild type or laboratory grown frogs by surgical procedures or by sacrifice of the frog. An adult frog can produce approximately 40000 oocytes that are at various stages of development. Fully-grown oocytes consist mainly of yolk proteins obtained from the maternal circulation and translation components required for the synthesis of proteins after fertilisation. Among these are three RNA polymerases sufficient to support zygotic transcription (Matthews, 1999). The oocytes grow to a diameter of >1mm and are visible with the naked eye. The ovaries of a mature female frog contain oocytes stretching over six different stages (I-VI, Figure 3.2B). Only the last two stages (stages V and VI) are used in expression studies. Stage V and VI stage cells are from 1-1.3 mm in diameter and with a light vegetal pole and a darker animal pole, which contains the nucleus. Less mature cells can be identified by the lack of pole differentiation and a uniform grey to white pigmentation. A good *Xenopus* specimen will normally contain ≥70% of stage V and VI oocytes. Under the right conditions the harvested oocytes can survive for a week and express proteins within 24h (Smart and Krishek, 1995; Yao *et al*, 2000).

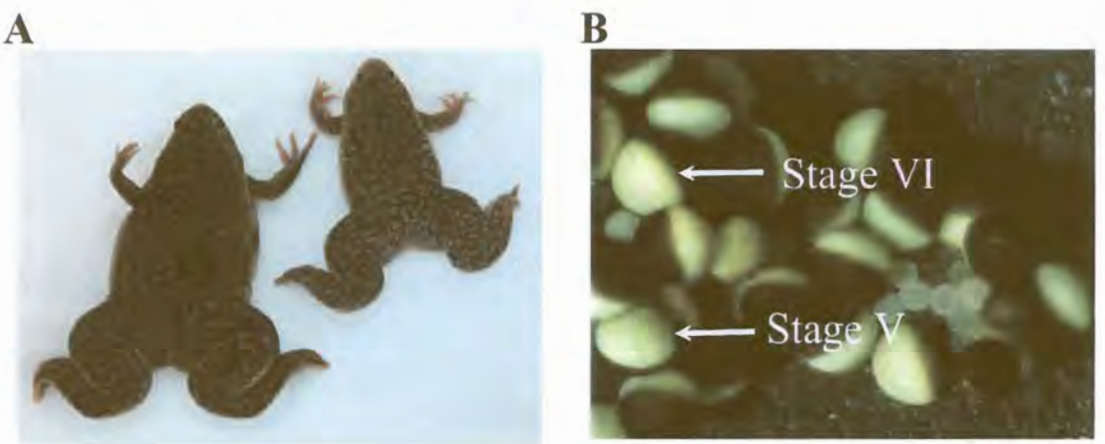

Figure 3.2: The *Xenopus laevis* frog and oocytes. Figure A demonstrates the morphology of the *Xenopus laevis* clawed frog. **Figure B** shows a typical mixture of *Xenopus* oocytes at various stages of development. The stage V oocyte is characterised by defined hemispheres. The stage VI oocyte can be distinguished from stage V by an equatorial band between the two phases. The colour of the mature oocytes can range between grey, brown, yellow and green (Yao *et al*, 2000).

The *Xenopus* oocyte expression system has been used for the heterologues expression of proteins from several different species. Heterologous expression of *P. falciparum* proteins is difficult because of *Plasmodium's* codon preferences and high A+T content (Withers-Martinez *et al*, 1999). However, the *Xenopus* oocyte expression system has been used successfully for the expression of *P. falciparum* proteins. The first reported use of this system for *P. falciparum* proteins dates back to 1982 (Gritzmacher and Reese, 1982).

Since then the successful expression of the ATP-binding cassette transporter, pfmdr1 (van Es *et al*, 1994), nucleoside, nucleobase, hexose and monocarboxylate transporter systems (Penny *et al*, 1998), as well as two different nucleoside/nucleobase transporters in *X. laevis* oocytes were reported (Parker *et al*, 2000; Carter *et al*, 2000). The isolation and expression of the *P. falciparum* hexose transporter PfHT1 in *Xenopus* oocytes was first described in 1999 (Woodrow *et al*, 1999).

Vectors such as pGEM-3Z (Promega) or pBluescript (Stratagene) are generally used for expression in *Xenopus* oocytes, but for the difficult malarial proteins it is recommended to use expression vectors such as pSP64T (Kreig and Melton, 1984) or pGEM-HE (Liman *et al*, 1992). The pSP64T vector contains an Ampicillan resistant gene, an SP6-promoter site and unique *Hind*II and *Bgl*II restriction sites situated between the 5'- and 3'-untranslated regions of the *Xenopus* β-globin gene (Appendix Ia; Yao *et al*, 2000). Studies conducted by Woodrow *et al* (2000) demonstrated the benefit of these untranslated regions as opposed to the same vector lacking them. In their work, they also included a Kozak sequence directly in front of the start codon (e.g. mRNA 5' – ACCAUG where the start codon is underlined), which is thought to be recognised by the ribosomal subunit at the start of synthesis (Lodish *et al*, 1995). In the absence of these additions, synthesis of the PfHT1 transporter was low as indicated by glucose uptake. Synthesis increased slightly with the inclusion of the 5'- and 3'-untranslated regions, and increased even more so with just the Kozak consensus in front of the PfHT1 start codon. However, inclusion of both the untranslated regions and the Kozak sequence produced the highest synthesis of transporter (Figure 3.3; Woodrow *et al*, 2000).

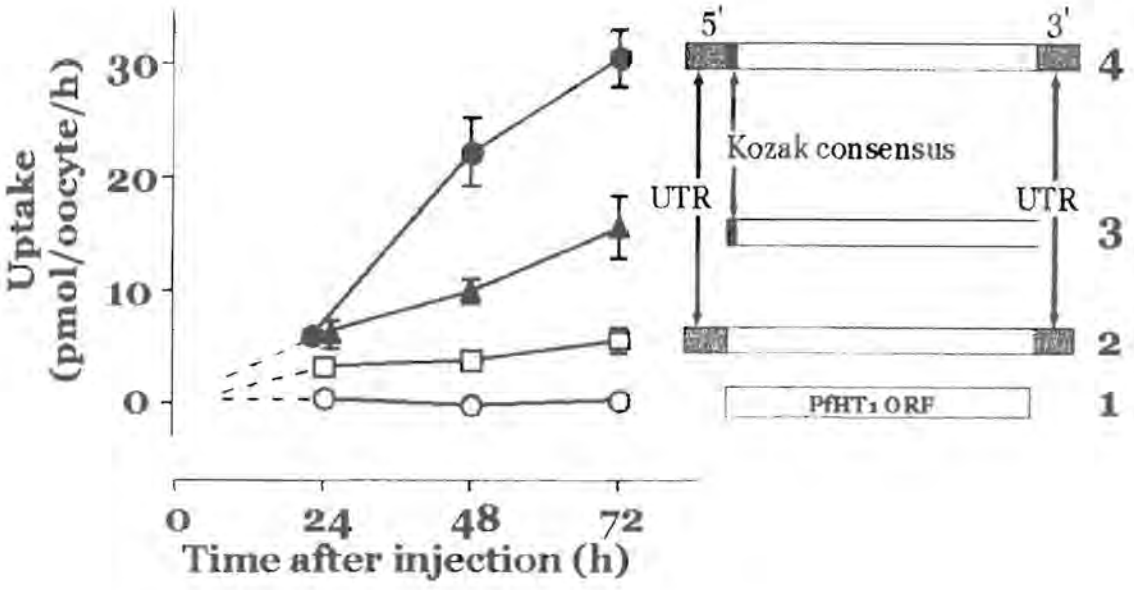

Figure 3.3: Influence of untranslated region (UTR) from *Xenopus* β-globin, and Kozak on expression of PfHT1 in *Xenopus* oocytes. ○ (1) = PfHT1 ORF. □ (2) = PfHT1 ORF UTR. ▲ (3) = PfHT1 ORF with the Kozak consensus. ● (4) = PfHT1 ORF with both the UTR and Kozak consensus (Woodrow *et al*, 2000).

In the present study three helix 7 mutant glucose transporters (described in Chapter 2) contained in the pSP64T vector namely, mutants SGL→AGT (denoted XF2.4), SGL→AGL (denoted XA1.4) and SGL→SGT (denoted XT1.10) were used as templates for synthesis of cRNA (Paragraph 2.2.9). Also included was a helix 5 mutant (denoted XmaI, described in Paragraph 2.4). Synthesised cRNA was injected into *Xenopus* oocytes and used for the estimation of kinetic parameters K_m (affinity or Michaelis constant) and K_i (half-maximal inhibition constant for carrier transport) for D-glucose and D-fructose. Estimations of K_i values for glucose analogues were also determined for each mutation. The latter kinetic parameters assist in the interpretation of the PfHT1 protein-substrate interactions.

3.2 Materials and methods

3.2.1 Harvesting of *Xenopus* oocytes

Harvesting of the *Xenopus* oocytes was conducted by two separate methods, one of which involved the sacrifice of the frog and the other one the anaesthetisation of the frog.

3.2.1.1 *Sacrifice of* Xenopus laevis

A mature female frog was placed in ice water for approximately 90 minutes to subdue her. The frog was removed from the water and decapitated by guillotine and placed dorsal side up on the operating surface. The sacs of oocytes were removed from the frog via an incision in the lower abdomen. All possible oocytes were removed to obtain maximum yield. The frog was disposed of in the appropriate manner (S. Krishna and C. J. Woodrow, personal communication). The oocytes were placed in a Petri dish containing calcium free Ringer solution (0.08 M NaCl, 1.3 mM KCl, 0.3% w/v N-2-hydroxylethylpiperazine-N'-2-ethanesulfonic acid (HEPES), pH 7.6; Smart and Krishek, 1995).

3.2.1.2 *Anaesthesia of* Xenopus laevis

A mature female frog was selected and placed in a separate container in tap water. A solution of 0.2% w/v MS-222 (3-Aminobenzoic Acid Ethyl Ester or Tricaine, Sigma, cat no A5040) was made up with 5 mM Tris-HCl (pH 7.4). This was placed in a glass container and the frog immersed in it. The degree of anaesthesia was checked every 5 minutes by turning the frog dorsal side up and checking for the "righting-reflex". Once anaesthetised the frog was washed under tap water to remove traces of anaesthetic. The frog was then placed dorsal side up on a flat bed of ice in a shallow tray. All bench surfaces were swabbed with 70% v/v ethanol and all surgical instruments were sterilised by autoclaving or with 70% v/v ethanol prior to operating. A small incision (1 cm) was made with a scalpel through the outer layer of the skin on one side of the frog. Another incision was then carefully made through the connective tissue and muscle sheet. Damage to the internal organs was avoided by lifting the exposed muscle sheet with a pair of forceps. Using a pair of forceps a section of ovary

sac-containing oocytes was carefully teased out of the incision. The sac was pinched off using absorbable surgical sutures and the oocytes were removed with scissors. The oocytes were placed in a Petri dish containing calcium-free Ringer solution. The incision was kept clear of blood and oocytes by constant spraying with distilled water and the skin and muscle layers were stitched separately using absorbable suture. The frog was recovered in a sloped container in distilled water containing 0.5% w/v NaCl for 12 hours and then left in distilled water until being returned to it's tank (Dr Eckstein-Ludwig, St. Georges Hospital Medical School, London, personal communication; Smart and Krishek, 1995).

3.2.2 Preparation of *Xenopus* oocytes

The oocytes contained in the Petri dish with calcium-free Ringer solution were manually separated into clumps with forceps and scissors. The oocytes were repeatedly washed in calcium-free Ringer solution to remove all traces of blood and cytoplasm from any ruptured oocytes. The oocytes were then defolliculated by treatment with 2 mg/ml collagenase (0.2-0.5 U/ ml, type 1A, Sigma-Aldrich, USA) for 60-120 minutes at room temperature on a shaker at approximately 50 rpm. After complete separation of the oocytes was obtained the collagenase reaction was stopped with Barth's solution (0.08 M NaCl, 1.3 mM KCl, 0.3% w/v HEPES, 0.32 mM $Ca(NO_3)_2$, 0.04 mM $CaCl_2$, 0.8 mM $MgSO_4$, 0.2% w/v $NaHCO_3$, pH 7.6; Smart and Krishek, 1995). The oocytes were repeatedly washed in Barth's solution to remove all traces of collagenase and then stored in Barth's solution containing 0.01 mg/ml penicillin and 0.01 mg/ml streptomycin (Sigma, UK) and incubated at 19°C until use.

3.2.3 Selection of *Xenopus* oocytes

Oocytes at stage V and VI were selected using a blunt and fire polished Pasteur pipette with the aid of a dissection microscope and a fibre optic lamp. Stage V and VI oocytes that had a distinct separation between the dark animal pole and light vegetal pole and without any discolouration or lesions or protrusions were selected. The much smaller and lighter Stage I oocytes, which can make selection more difficult, were

removed by repeated agitation and settlement of the oocytes in a 50 ml tube. The Stage I oocytes settled slower and were removed by vacuum suction or decanting without damage to any of the other cells. Selected stage V and VI cells were placed in a clean Petri dish containing Barth's solution with 0.01 mg/ml penicillin and 0.01 mg/ml streptomycin and incubated at 19°C until microinjection.

3.2.4 cRNA for microinjection into *Xenopus* oocytes

cRNA was prepared as described in Paragraph 2.2.9. The cRNA used for microinjections included that from wild type (PfHT1, provided by S. Krishna, St. George's Hospital Medical School, London) and the three helix 7 mutants namely, the SGL→AGT mutant (denoted XF2.4), the SGL→AGL mutant (denoted XA1.4) and the SGL→SGT mutant (denoted XT1.10). Also included in the cRNA pool was a helix 5 mutant provided by C. J. Woodrow (Woodrow *et al*, 2000). This mutant contains a point mutation at amino acid 169 (Q169N) and is denoted XmaI. No prior kinetic analysis of the helix 5 mutant had been performed other than determination of its K_m for D-glucose (Woodrow *et al*, 2000).

3.2.5 Microinjection of *Xenopus* oocytes

Sets of ten to twenty oocytes were drawn up in a blunt and fire polished Pasteur pipette and positioned on an oocyte holder (designed by S. Krishna, St. Georges Hospital Medical School, London) or in between two overlapping glass slides under a dissecting microscope illuminated by a fibre optic lamp. Glass capillaries were pulled into needles using a PUL-1 capillary puller (World Precision Instruments, UK) followed by attachment to the micromanipulator connected to a PicoPump microinjector (PV830) with PicoNozzle (World Precision Instruments, UK). RNA samples previously stored at -70°C were thawed on ice and diluted with nuclease-free water to concentrations of 0.4-0.5 ng/nl and pipetted onto parafilm. The RNA was drawn up into the needle by a suction pump attached to the microinjector. Volumes of 25-30 nl of RNA were injected into the vegetal pole of each oocyte if possible.

Alternatively RNA samples were diluted with nuclease-free water to concentrations of 2 ng/nl. The RNA was drawn up into an Eppendorf Microloader (Eppendorf, Germany) and pipetted into sterile Femtotips II (Eppendorf, Germany). The Femtotip was then connected to an Eppendorf FemtoJet microinjector (Eppendorf, Germany) and stabilised on a micromanipulator. Oocytes were injected with volumes of 5-7 nl RNA solution at a time.

Positive controls included oocytes injected with equal concentrations of wild type PfHT1 RNA or mammalian rat glucose transporter GLUT1 RNA (provided by S. Krishna, St. Georges Hospital Medical School, London), and negative controls or backgrounds were nuclease-free water-injected oocytes. Injected oocytes were collected in a Petri dish containing Barth's solution and antibiotics and incubated at 19°C for 1-4 days.

3.2.6 Uptake studies

Uptake measurements were conducted at intervals of 24, 48 and 72 hours after microinjection. Approximately 50 oocytes were injected for each cRNA and for each control (PfHT1 as positive control and water as negative control). At each time interval 6-8 oocytes were selected from each cRNA injected batch and 6 oocytes from the positive and negative controls. Oocytes were incubated in Barth's solution containing 2.5 µM D-[U-^{14}C]-glucose (Amersham Life Sciences, UK, 323 mCi/mmol) and 30 nM D-glucose (Sigma, UK) for 20 minutes and then washed three times in ice cold Barth's solution. Single oocytes were transferred into either a 1.5 ml microfuge tube and then counted on a Wallac 1450 Microbeta Plus scintillation counter (Wallac, Milton Keynes, UK) or in a 5 ml polyethylene Pony Vial (Packard, USA) and counted on a Minaxiβ Tri-Carb 4000 series liquid scintillation counter (United Technologies Packard, USA). 2 µl of uptake solution was also counted for each experiment and used to calculate pmol/ oocyte/ hour similar to calculations described in Paragraph 3.2.8. Uptakes were measured as decay per minute (DPM). Results were transferred into Microsoft Excel tables from which graphs were plotted to compare glucose uptakes for cRNA-injected and control-injected oocytes at each time interval.

3.2.7 Kinetic Assays

Once transport had been established for the mutant glucose transporters, the K_i and K_m values were determined. This analysis usually took place 36-48 hours after microinjection when expression was high and degradation of the oocytes was low. The uptake solutions used to determine the K_m for D-glucose of the mutant transporters contained 2.5 μM D-[U-^{14}C]-glucose (Amersham Life Sciences, UK, 323 mCi/mmol) in Barth's solution (pH 7.4) and 0.2-2 mM D-glucose. The uptake solutions used to determine the K_m for D-fructose of the mutant transporters contained 5.6 μM D-[U-^{14}C]-fructose (Amersham Life Sciences, UK, 289 mCi. mmol^{-1}) in Barth's solution (pH 7.4) and 1-20 mM D-fructose. Uptake solutions used to determine the K_m for 2-deoxy-D-glucose (2-DOG) and 3-*O*-methyl-D-glucose (3-OMG) contained 14.3 μM 2-deoxy-D-[U-^{14}C]glucose (58 mCi.mmol^{-1}) or 16.6 μM 3-*O*-[^{14}C]methyl-D-glucose (50 mCi.mmol^{-1}; Amersham Life Sciences, UK) in Barth's solution (pH 7.4) and 0.3-20 mM 2-DOG or 0.2-10 mM 3-OMG, respectively.

Six sets of different concentrations were used per K_m determination with 8 RNA and 6 water injected oocytes per set. Oocytes were immersed in uptake solution for 20 minutes, then removed and washed three times in ice-cold Barth's solution.

For each K_i analysis a total of 50-100 oocytes were injected with cRNA and 30-80 oocytes with water. Eight cRNA injected oocytes were used for either glucose analogues, D-fructose or the fructose analogue, 2,5-anhydro-D-mannitol (2,5-AHM) at five different concentrations each. Included in each experiment was one set of 8 cRNA injected oocytes incubated in only D-glucose (uninhibited) and a set of 6 water injected oocytes. Each uptake solution for K_i analysis contained 2.5 μM D-[U-^{14}C]-glucose and 30 nM D-glucose in Barth's solution and a range of concentrations of glucose analogues, D-fructose and 2.5-AHM. Glucose analogues included 1-deoxy-D-glucose (1-DOG), 2-deoxy-D-glucose (2-DOG), 3-*O*-methyl-D-glucose (3-OMG), 5-thio-D-glucose and 6-deoxy-D-glucose (6-DOG). D-fructose and all analogues were from Sigma or Amersham (Sigma-Aldrich, UK; Amersham, UK; Figure 3.4). Each oocyte was placed in a separate microfuge tube or pony vial and lysed in the appropriate volume of scintillation fluid and counted in a scintillation counter.

Glucose analogues

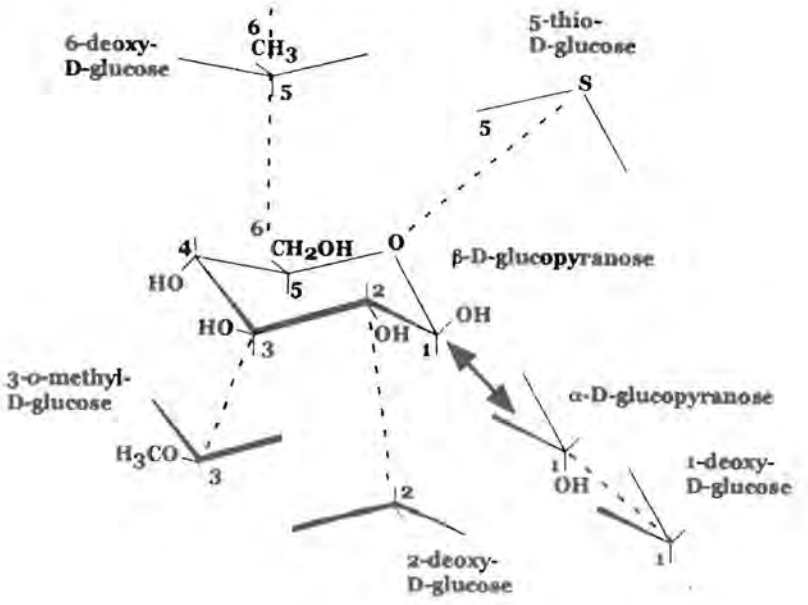

Fructose analogues

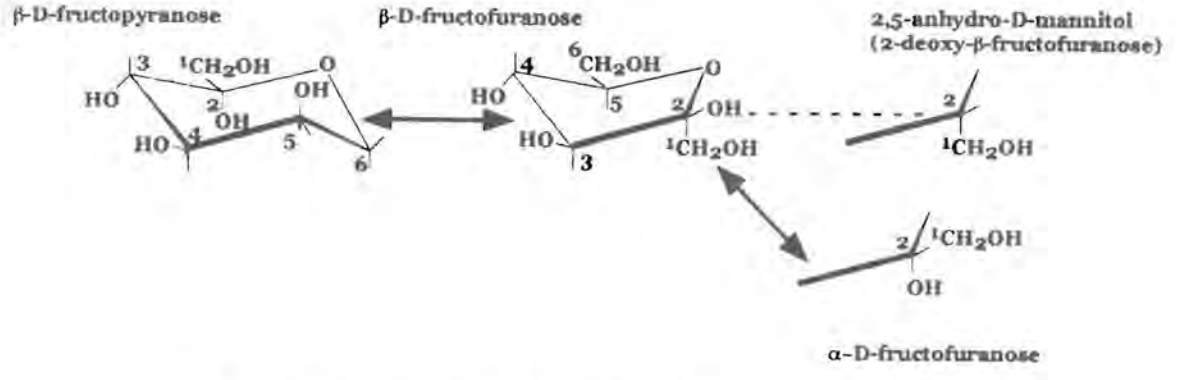

Figure 3.4: Analogues used in studies on PfHT1 and the mutated transporters Xma1, XF2.4, XA1.4 and XT1.10. Structures are represented as chair conformations. Solid arrows indicate conversions that occur under normal conditions in solution.

3.2.8 Data analysis

Initial DPM results from K_m and K_i experiments were transferred into Microsoft Excel tables to calculate the pmols/ oocyte/ hour (for K_m) and percentage of uninhibited transport (for K_i). These values were used to calculate the K_m and K_i with Prism version 2.0 (GraphPad Prism inc., USA). A Michaelis-Menten model was used for all

estimations of kinetic parameters by nonlinear regression analysis. The pmol/ oocyte/ hour value is calculated as follows:

A volume (2 µl or $2/10^6$ L) of uptake solution was counted and determined as DPM (C). *With the known concentration of inhibitor in mM* (A) *the DPM data obtained for each oocyte* (B) *was then used to determine the pmols of substrate transported into each oocyte.*

$$\frac{2\cancel{L}}{10^6} \times \frac{\text{A mmols}}{\cancel{L}} \times \frac{\text{B } \cancel{\text{DPM}}/\text{ oocyte}}{\text{C } \cancel{\text{DPM}}}$$

$\therefore 2/10^6 \times A \times B/C$ mmols/ oocyte

To get pmols: $2/10^6 \times A \times B/C$ *mmols/ oocyte* $\times 10^9$

$\therefore 2 \times 10^3 \times A \times B/C$ pmols/ oocyte

Each uptake is performed for a certain time D *(eg. 20 minutes). The time is taken as a fraction of an hour,* 60/D.

$\therefore 2 \times 10^3 \times A \times B/C \times 60/D$ pmols/ oocyte/ hour

3.3 Results

3.3.1 Uptake studies

The time course of glucose uptake induced by PfHT1 or the 302SGL→AGT, S302A and L304T PfHT1 helix 7 mutants are shown compared in Figure 3.5. Reconfiguration of the 302SGL triplet motif in helix 7 of PfHT1 to an equivalent motif (AGL) found in THT1, the *T. brucei* hexose transporter, appeared to alter the overall uptake rates of ^{14}C-glucose when compared with the wild type PfHT1 transporter 72 hours after microinjection ($P < 0.012$, n = 2, where values below 0.05 are considered statistically significant, see Figure 3.5 for an example of one experiment out of the three that were conducted.). In the example shown in Figure 3.5, the expression or efficiency of XF2.4 (the 302SGL→AGT mutant) was clearly delayed or lower compared with the wild type at 24 ($P < 0.0001$), 48 ($P < 0.0001$) and

72 ($P = 0.012$) hours after microinjection. XF2.4 produced uptake measurements that were below half that of the wild type PfHT1 at 24 hours after microinjection (25.0 ± 2.7 pmols/ oocyte/ hour compared with the wild type at 63.6 ± 4.4 pmols/ oocyte/ hour), and over half at 48 hours after microinjection (42.3 ± 2.4 pmols/ oocyte/ hour compared with the wild type at 77.4 ± 5.9 pmols/ oocyte/ hour) and 72h after microinjection (29.6 ± 4.1 pmol/ oocyte/ hour compared with the wild type at 56.7 ± 8.4 pmol/ oocyte/ hour). Uptake measurements plateau after 72h (results not shown).

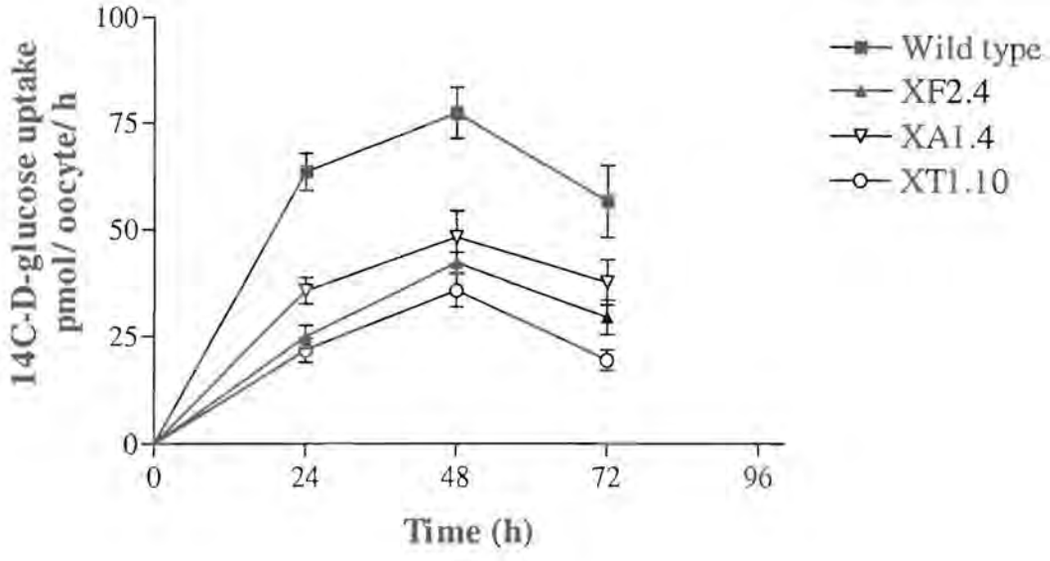

Figure 3.5: Time course assay of helix 7 mutants XF2.4, XA1.4 and XT1.10 compared with the wild type PfHT1. An equal concentration of cRNA from the wild type and each mutant was injected per oocyte. Glucose uptakes were assayed at the times indicated. Eight oocytes were used per uptake. Data displayed are mean ± SE of eight oocytes.

Uptake measurements for the time study were carried out on the S302A (XA1.4) and L304T (XT1.10) mutants in order to better define which amino acid within the XF2.4 construct was most responsible for the lower uptake measurements seen at 24, 48 and 72 hours (Figure 3.5). Uptake measurements with D-glucose proved each construct to be functional. Both XA1.4 and XT1.10 showed lower uptake ($P < 0.0010$) than the wild type at 24 hours (35.8 ± 3.1 pmol/ oocyte/ hour and 21.8 ± 2.8 pmol/ oocyte/ hour, respectively) and 48 hours (48.3 ± 6.2 pmols/ oocyte/ hour and 35.9 ± 3.9

pmols/ oocyte/ hour, respectively) after microinjection. The XA1.4 mutant had uptake values higher than XT1.10 at 24 and 48 hours after microinjection. At 72 hours the mean uptake value for XA1.4 shown in Figure 3.5 (37.8 ± 5.3 pmol/ oocyte/ hour) was not significantly different (P = 0.0780) compared with the wild type, but was significantly different (P = 0.0069) compared with XT1.10. The mean uptake measurements for XA1.4 were only significantly different to XF2.4 at 24 hours in 2 of the 3 independent experiments. The mean uptake values for XT1.10 were not significantly different to XF2.4 at any time point in 3 independent experiments.

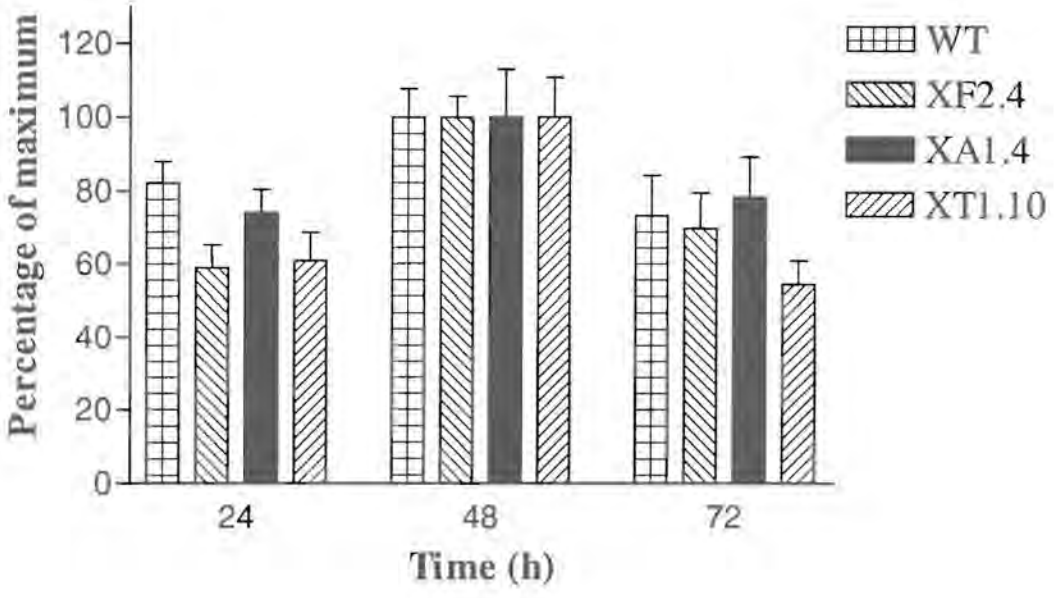

Figure 3.6: Normalization of the results represented in Figure 3.5. Values are shown as percentages of the maximum expression, which is taken at 48 hours, for each mutant and the wild type independent of each other. Data displayed are mean ± SE of eight percentages from each of the eight oocytes from Figure 3.5.

With the results in Figure 3.5 normalized as shown in Figure 3.6, it can be speculated that the XA1.4 mutant may follow a similar expression pattern to the wild type. Maximum expression is seen at 48 hours which is taken as 100%. At 24 hours XA1.4 shows 74.1 ± 6.4% of its maximum expression and the wild type is at 82.2 ± 5.7 %. At 72 hours XA1.4 shows 78.3 ± 10.9 % of its maximum expression and the wild type is at 73.3 ± 10.9 %. The XT1.10 mutant follows a similar expression pattern to that of

XF2.4. At 24 hours XT1.10 shows 60.9 ± 7.8 % of its maximum expression and XF2.4 is at 58.9 ± 6.4 %. At 72 hours XT1.10 shows 54.4 ± 6.5 of its maximum expression and XF2.4 is at 69.8 ± 9.6 %. In subsequent experiments, similar patterns were seen between the wild type and the mutants.

3.3.2 Kinetics of substrate transport of mutants in comparison to PfHT1

Table 3.1 provides K_m and K_i values obtained for PfHT1 and its various mutants. The K_m values indicate the affinity between PfHT1 and substrate. To characterise substrate-transporter interactions, a series of hexose analogues are used as competitors for transport of D-glucose, which provides a K_i value for each analogue. Uptake experiments for K_m studies involve a homogeneous solution of substrate and the rate of uptake is uniform. Uptake experiments for K_i studies involve a heterogeneous solution containing competitor (analogues) and substrate (glucose). The rate of translocation of the substrate compared with the competitor may differ; therefore K_i values are only estimates of affinity between PfHT1 and competitor.

The mutation of helix 7 SGL motif to AGT (XF2.4) supports transport of both D-glucose and D-fructose. The affinity of D-glucose for XF2.4 is not significantly different to that of the wild type ($P = 0.4825$). The affinity of glucose for XF2.4 (K_m = 0.95 ± 0.2 mM) is similar to that of the wild type (K_m = 1.0 ± 0.2 mM). XF2.4 was also capable of transporting 1-DOG, 2-DOG, 3-OMG, 5-thio-D-glucose and 6-DOG (Table 3.1). The segregated mutants S302A (XA1.4) and L304T (XT1.10) show a similar ability to transport D-fructose and D-glucose as well as the glucose analogues mentioned above. The increased affinity of glucose for the XA1.4 mutant (K_m = 0.47 ± 0.1 mM) was significantly different from the wild type ($P = 0.0410$) but not from the XF2.4 mutant ($P = 0.0600$). The increased affinity of glucose for the XT1.10 mutant (K_m = 0.68 ± 0.04 mM) was not significantly better ($P = 0.0887$) than the wild type, nor the XF2.4 mutant ($P = 0.1680$). The results therefore suggest a higher affinity of the XA1.4 for glucose to that of the wild type. The helix 5 mutant Q169N, though unable to transport D-fructose as previously reported (Woodrow *et al*, 2000), was capable of transporting D-glucose and the glucose analogues mentioned above.

3.3.2.1 Aldose analogue analysis

3.3.2.1.1 Deoxyaldose analogues.

Helix 5 mutant: For the helix 5 Q169N mutant (Xma1) the results in Table 3.1 indicate no change in affinity for 1-DOG (K_i = 13.6 ± 2.0 mM) compared with the wild type (K_i = 14.7 mM, 15.9 mM). A significant 2-3-fold decrease (P = 0.0045) in affinity was observed for 2-DOG (K_m = 3.4 ± 0.3 mM) compared with wild type (K_m = 1.3 ± 0.4 mM). A significant 3-4-fold decrease (P = 0.0087) in affinity was observed for 6-DOG (K_i = 7.9 ± 0.8 mM) compared with wild type (K_i = 2.2 ± 0.9 mM). An approximate 4-fold and significant increase (P = 0.0062) in affinity for 5-thio-D-glucose was shown for Xma1 (K_i = 0.8 ± 0.1 mM) compared with the wild type (K_i = 2.9 ± 0.4 mM).

Helix 7 mutants: DOG studies on the helix 7 mutant (302SGL→AGT; XF2.4) revealed a 2-fold decrease in affinity for 1-DOG (K_i = 26.4 ± 1.1 mM), and a 3-fold decrease in affinity for 6-DOG (K_i = 6.8 ± 1.0 mM), which are statistically significant (P = 0.0048 and 0.0273, respectively). However, its affinity for 2-DOG (K_m = 1.2 ± 0.5 mM) remained the same as the wild type. A 5-fold and significant decrease (P = 0.0039) in affinity was observed for 5-thio-D-glucose (16.1 ± 2.2 mM) compared with the wild type. Kinetic studies on the point mutation S302A together with statistical calculations showed that the 2-fold increase in K_i with 1-DOG observed for XF2.4 might be attributed to this single point mutation (K_i = 42.7 ± 5.4 mM, with P = 0.0301 when compared with the wild type) and not to the L304T mutation (K_i = 19.0 ± 2.1 mM, with P = 0.2729 when compared with the wild type). No statistically significant increase in K_i for 6-DOG was observed when compared with wild type for either S302A (K_i = 2.4 ± 0.2 mM; P = 0.9754) or L304T (K_i = 3.8 ± 0.7 mM; P = 0.2299). Both S302A and L304T mutants separately showed an increase in affinity for 5-thio-D-glucose (K_i = 11.2 ± 1.6 mM and 8.2 ± 2.0 mM) compared with the XF2.4 mutant but still a decrease in affinity compared with the wild type. Only the S302A mutant showed a statistically significant increase in affinity (P = 0.0067) for 5-thio-D-glucose when compared with the wild type. The K_i for 2-DOG obtained from XA1.4 (K_i = 0.7

± 0.2 mM) and XT1.10 (K_i = 1.2 ± 0.3 mM) was similar to the K_m value obtained from the wild type.

3.3.2.1.2 Methylaldohexoses.

The replacement of hydrogen with a larger methyl group gives an indication of the available space surrounding the carbon, and the proximity of the protein to the sugar at that site. The K_m values (7.3 mM, 5.5 mM) achieved with 3-OMG for the Q169N mutant indicated a significant decrease in affinity (P = 0.0067) of the mutant transporter for 3-OMG compared with the wild type (K_m = 1.3 ± 0.3 mM). The same is true for XF2.4 where the K_m result (K_m = 5.6 ± 0.8 mM) is 4-fold higher and significantly different (P = 0.0074) to that of the wild type. The K_i values for the XA1.4 and XT1.10 mutants for 3-OMG (K_i = 1.2 ± 0.2 mM and 1.0 ± 0.1 mM, respectively) were similar to that of the wild type (K_i = 1.4 mM, 2.7 mM; K_m = 1.3 ± 0.3 mM) and not significantly different (P = 0.6379 and 0.3553, respectively).

3.3.2.2 Ketose analogue analysis

As shown in Table 3.1 the Q169N mutant does not transport D-fructose in agreement with previously reported results (Woodrow *et al*, 2000). The mutations in helix 7 were also thought to play a role in fructose transport. For the helix 7 mutants, there appears to be a decrease in affinity for fructose as evidenced by the K_m values of all three mutants in comparison to the wild type. The XF2.4 mutant shows a 2-fold decrease in affinity (K_i = 23.1 ± 1.9 mM) and the segregated mutants XA1.4 and XT1.10 show a similar decrease (K_i = 19.9 ± 1.7 mM and 17.1 ± 3.0 mM, respectively) compared with the wild type (K_m = 11.5 ± 1.6 mM or $K_i \approx$ 11 mM). The decrease in affinity for fructose seen for XF2.4 was statistically significant (P = 0.0258) compared with the wild type, whereas XA1.4 and XT1.10 were not (P = 0.0.0630 and P = 0.2495, respectively). To confirm these results, transport of the fructose analogue 2,5-anhydro-D-mannitol (2,5-AHM) was also determined. All three helix 7 mutants XF2.4 (K_i = 1.7 ± 0.15 mM), XA1.4 (K_i = 2.2 mM, 1.2 mM) and XT1.10 (K_i = 2.7 mM, 1.0 mM) showed no significant difference in K_i for 2,5-AHM compared with the wild type (K_i = 1.4 ± 0.3 mM) with P values of 0.4791, 0.6532 and 0.6121, respectively.

Table 3.1: Kinetic analysis of helixes 7 and 5 mutants compared to the wild type on transport of glucose, fructose and analogues . All values are in mM. PfHT1 kinetic results have been previously reported (Woodrow, *et al*, 2000) except for one 5-thio-D-glucose value and one 1-DOG value, which were needed for a SE calculation. Xma1 is the Q169N mutant of helix 5 that has been previously reported but on which no kinetic studies had been done.

*Means ± SE of three independent experiments unless otherwise indicated.

†Xma1 glucose K_m and ketose analogue results were obtained from previous experiments (Woodrow, *et al*, 2000).

Substrate	PfHT1 (wild type)	*Helix 5 mutant* Xma1† (Q169N)	*Helix 7 mutant* XF2.4 (302SGL→AGT)	*Helix 7 mutant* XA1.4 (S302A)	*Helix 7 mutant* XT1.10 (L304T)
Aldose analogues D-glucose	$K_m = 1.0 \pm 0.2$*	†$K_m = 1.2 \pm 0.2$	$K_m = 0.93 \pm 0.3$	$K_m = 0.47 \pm 0.2$	$K_m = 0.68 \pm 0.07$
C1-position 1-deoxy-D-glucose	$K_i = 14.7, 15.9$	$K_i = 13.6 \pm 3.4$	$K_i = 26.4 \pm 1.9$	$K_i = 40.0 \pm 6.4$	$K_i = 19.0 \pm 3.7$
C2-position 2-deoxy-D-glucose	$K_m = 1.3 \pm 0.4$	$K_m = 3.4 \pm 0.5$	$K_m = 1.2 \pm 0.8$	$K_i = 0.7 \pm 0.3$	$K_i = 1.2 \pm 0.5$
C3-position 3-*O*-methyl-D-glucose	$K_m = 1.3 \pm 0.3$ $K_i = 1.4, 2.7$	$K_m = 7.3, 5.5$	$K_m = 5.6 \pm 1.6$ (n = 4)	$K_i = 1.2 \pm 0.4$	$K_i = 1.0 \pm 0.2$
C5-position 5-thio-D-glucose	$K_i = 2.9 \pm 0.7$	$K_i = 0.8 \pm 0.1$	$K_i = 16.1 \pm 3.7$	$K_i = 11.2 \pm 2.7$	$K_i = 8.1 \pm 3.3$
C6-position 6-deoxy-D-glucose	$K_i = 2.2 \pm 0.9$	$K_i = 7.9 \pm 1.5$	$K_i = 6.8 \pm 1.8$	$K_i = 2.4 \pm 0.4$	$K_i = 3.8 \pm 1.1$
Ketose analogues D-fructose	$K_m = 11.5 \pm 1.6$ $K_i = 10.6, 11.7$	†No trans.	$K_i = 23.0 \pm 3.2$	$K_i = 19.9 \pm 3.0$	$K_i = 17.1 \pm 5.2$
C2-position 2,5-anhydro-D-mannitol	$K_i = 1.4 \pm 0.3$	†$K_i = 28$	$K_i = 1.7 \pm 0.2$	$K_i = 2.2, 1.2$	$K_i = 2.7, 1.0$

3.4 Discussion

Three mutations in the PfHT1 helix 7 motif SGL and one in helix 5 (Q169N) were investigated. These two helices have previously been implicated in substrate binding or glucose/ fructose differentiation. The most significant difference up to date between the PfHT1 and GLUT1 transporters is PfHT1s ability to transport fructose as well as glucose (Woodrow *et al*, 1999). Studies with mammalian glucose transporters (GLUT1, 3 and 4) and hexose transporters (GLUT2 and 5) have implicated helix 7 as being involved in glucose/ fructose recognition and translocation (Arbuckle *et al*, 1996; Seatter *et al*, 1998). Cysteine-scanning mutagenesis studies on GLUT1 helix 5 have indicated 6 amino acids accessible to external medium all of which were clustered along one face of the putative α-helix (Mueckler *et al*, 1999). Similar studies were conducted with GLUT1 helix 7. Several amino acids in GLUT1 helix 7, predicted to lie near the exofacial side of the cell membrane, were shown to be accessible to outside medium. However these amino acids did not cluster along one face of the putative α-helix. This provided evidence for the likely positioning of helix 7 within the glucose permeation pathway as shown in Chapter 2, Figure 2.1B (Hruz and Mueckler, 1999).

In this study, the uptake measurements of the helix 7 and helix 5 mutants were performed on cRNA injected oocytes with D-glucose, D-fructose and hexose analogues. The XF2.4, XA1.4 and XT1.10 mutants produced lower uptake measurements compared with the wild type at 24, 48 and 72 hours (Figure 3.5). Since the K_m values for the helix 7 mutants are all similar to the wild type (Table 3.1), the lower uptake measurements seen at 24, 48 and 72 hours for XF2.4, XA1.4 and XT1.10 were not due to a decrease in affinity (Figure 3.5). Two possibilities exist that could explain this lower uptake. The mutations could be affecting the transporters ability to change its conformation, decreasing translocation of the substrate from the external medium to the inside (Chapter 1, Section 1.6.2.1), therefore the transporters efficiency is affected. If the mutant's ability to translocate substrate across the membrane is similar to the wild type, the lower uptake measurements could be as a result of a lower expression of the mutant transporters compared with the wild type so

that there are less mutant transporters compared with wild type transporters present on the membrane at any given time.

Since the XF2.4 mutant, which contains a double point mutation, was segregated into two single mutations S302A (XA1.4) and L304T (XT1.10), one may be able to determine if a single amino acid within the XF2.4 construct was responsible for the lower uptake seen for the mutant at 24, 48 and 72 hours. As shown in Figure 3.5, both the S302A and L304T mutants had similar uptakes to the XF2.4 mutant at 24, 48 and 72 hours after microinjection. However, the XT1.10 mutant had significantly lower ($P < 0.04$) uptakes than the XA1.4 mutant at 24, 48 and 72 hours. The expression patterns shown in Figure 3.6 suggest that the XA1.4 mutant follows a similar expression pattern to the wild type whilst the XT1.10 mutant follows a similar expression pattern to the XF2.4 mutant. This suggests that the L304T mutant may be in some way more responsible for the lower uptakes seen in Figure 3.5. However, both mutants collectively appear to have an effect on the transporters efficiency or expression. These results were reproducible in two further experiments.

For the kinetic studies (Paragraph 3.3.2), results obtained with glucose analogues with PfHT1 mutants were also compared with results obtained for the wild type to see what influence the mutation had over the already existing changes in affinity produced by the glucose analogues. These changes in affinity between mutant transporters and substrate will give insight into how a specific amino acid interacts with different carbon atoms on the glucose substrate. Those analogues that produced statistically significant changes in affinity are discussed below.

Deoxy-D-glucose (DOG) analogues provide insight into which ones out of the six possible hydrogen bonding sites on glucose are required for substrate-protein interactions via hydrogen bonds. These potential hydrogen-bonding sites are interrupted by removal of the hydroxyl group (on carbons 1-4 and 6) and by replacing the oxygen on C-5 with a sulphur atom. K_m is an indication of affinity between transporter and substrate. K_i is similar to K_m but provides only an estimate of affinity between transporter and substrate as discussed in Paragraph 3.3.1.

Looking at the helix 5 mutant (Q169N) in comparison with the results obtained for the wild type (Woodrow *et al*, 2000), Q169 did not appear to be involved in binding to the C-1 oxygen, as the K_i was no different to that obtained for the wild type. A statistically significant decrease in affinity was observed for 2-DOG, which suggests that the oxygen at this carbon is involved in hydrogen bonding to the helix 5 Q169 amino acid. The 3-DOG analogue was not used, but the 3-OMG analogue did produce a 5-fold decrease in affinity compared with the wild type, which is discussed below. A 4-fold increase in affinity between XmaI and 5-thio-D-glucose was produced, which could suggest that asparagine in helix 5 hydrogen bonds more strongly to the C-5 sulphur of 5-thio-D-glucose than the glutamine did that it replaced (Appendix II for amino acid structures). Both oxygen and sulphur have an equal potential to form hydrogen bonds as a result of an equal number (2) of lone-pair (valence) electrons. Sulphur differs to oxygen in that it is able to form a further 4 covalent bonds as a result of its empty 3d orbital in its outer electron shell. Whether this has caused the increase in affinity between XmaI and 5-thio-D-glucose is uncertain. A 4-fold decrease in affinity compared with the wild type was observed with 6-DOG, which suggests an importance for the C-6 hydroxyl group for hydrogen bonding to helix 5.

The introduction of a much larger methyl group on D-glucose C-3 gives an indication of the available space surrounding the carbon, and the proximity of the protein to the sugar at C-3. A 5-fold decrease in affinity between XmaI and 3-OMG compared with the wild type and 3-OMG was observed. This suggests that introduction of an asparagine in place of a glutamine (Q169N) decreased the ability of the transporter to transport 3-OMG. This is interesting since asparagine is one C-atom shorter than glutamine, which is expected to create more space for the accommodation of the methyl group. The introduction of a methyl group also increases the potential for hydrogen bonding. The higher potential for hydrogen bonding could increase the affinity of the transporter for the substrate. However, since affinity decreased instead, this is not the case. The additional hydrogens, introduced by 3-OMG, also increase the positive charge at C-3, which could have an adverse affect on the affinity of the transporter for the substrate. The relevance of glutamine in spatial interactions with 3-OMG can only be resolved by mutating it to larger residues such as arginine, lysine or histidine.

The results obtained for Q169 seem to indicate that this amino acid is important for hydrogen bonding to C-2, C-3, C-5 and C-6. However, when this amino acid was mutated to asparagines it resulted in the ablation of fructose transport. Therefore the importance of this amino acid in interactions with the substrate could be extensive, and hence it is probable that it interacts with the glucose substrate at all these carbon atoms.

For the helix 7 mutants, the S302 amino acid may be involved in hydrogen bonding to C-1, which when mutated to alanine decreases the affinity between PfHT1 and 1-DOG by almost a third (Table 3.1). Studies on the double mutation in helix 7 (302SGL→AGT; XF2.4) suggested an importance of C-6 (3-fold decrease in affinity with 6-DOG). However the affinity is not affected when the XF2.4 mutant is segregated into XA1.4 and XT1.10, which have K_i values similar to the wild type. Therefore the importance of D-glucose C-6 in hydrogen bonding to helix 7 at this motif is debatable, or perhaps both mutations need to be present for transport to be affected negatively. There is a 6-fold decrease in affinity between XF2.4 and 5-thio-D-glucose compared with the wild type. However, it appears that both amino acids (302S and 304L) may be needed for the helix 7 interactions with D-glucose substrate at C-5. Both separately cause a decrease in affinity for substrate when mutated, but only the S302A mutation causes a statistically significant decrease in affinity when compared with the wild type. Therefore the S302A mutant is probably more responsible for the decrease in affinity seen between XF2.4 and 5-thio-D-glucose. Oxygen is more flexible around its covalent bonds and therefore will allow the glucose to be more flexible to fit into the transporters binding site. Therefore the introduction of a sulphur atom at this site may cause the glucose to be more rigid and unable to interact properly at this helix 7 site within the transporter.

There is a 4-fold decrease in affinity between XF2.4 and 3-OMG compared with the wild type. The amino acids alanine and threonine that replace serine (S302) and leucine (L304), respectively, are shorter by one carbon. For S302A there is a loss of a hydroxyl group, which may have formed a hydrogen bond to the substrate at C-3. For the L304T mutant there is a gain of a hydroxyl group, which might interfere

negatively as a result of the increase in positive charges created by the additional hydrogens from the methyl group. As for their properties, S302A results in the exchange of a polar side chain to a non-polar side chain, and L304T results in the opposite. When these two mutations are separated the decrease in affinity is abolished, the reasons for which are unclear. Therefore both are needed for the decrease in affinity to occur between XF2.4 and 3-OMG.

Previous studies with PfHT1 showed hydrogen bonding to glucose to be important at position C-1 and C-3 with a more than 10-fold increase in K_i with 1-DOG and 3-DOG compared with D-glucose (Woodrow *et al*, 2000). The results of this study on helix 7 with glucose analogues suggest possible hydrogen-bonding interactions of the SGL motif with D-glucose C-1, C-3, C-5 and C-6. However, there are a few points to be considered when reviewing the results from this study. The decrease in affinity seen for XF2.4 and 3-OMG might not be as a result of loss of hydrogen bonding but rather as a result of disfavour of the transporter for the larger methyl group. Also, when the amino acids S302 and L304 were tested separately with 3-OMG, the decrease in affinity observed with XF2.4 was not reproduced. Therefore, the importance of glucose C-3 in hydrogen bonding might be better resolved with an analogue such as 3-DOG where the oxygen is absent. C-6 investigated with 6-DOG only produced a change in the double point mutation XF2.4 and not when the mutations were separated. This questions the validity of the decrease in affinity between XF2.4 and 6-DOG. Overall, when looking at the degree to which affinity was affected by the different analogues, it appears that C-1 and C-5 are more important in hydrogen bonding to helix 7.

GLUT1 helix 7 has previously been suggested by Arbuckle *et al* (1996) to be important in fructose transport. Therefore it was hypothesised that the PfHT1 SGL motif in helix 7 could be important for D-fructose transport, and that mutation of this motif might affect affinity for D-fructose. PfHT1 transports D-fructose only in its furanose form, and a strong inhibitor of D-fructose is 2,5-anhydro-D-mannitol (2,5-AHM), which is fixed in the furanose form and differs from D-fructose only in the absence of a 2-hydroxyl group. The use of this fructose analogue provides a good indication of the ability of the helix 7 mutants to transport D-fructose. Only one of the

helix 7 mutant constructs (XF2.4) showed a statistically significant decrease in affinity (P = 0.0258) for D-fructose compared with the wild type. However, all three helix 7 mutants (XF2.4, XA1.4 and XT1.10) showed no difference in affinity for 2,5-AHM compared with the wild type. Therefore it cannot be said for certain that these helix 7 mutations have any affect on the transport of fructose.